Montana Precipitation Isotope Network (MTPIN): 4-Year Stable Water Isotope Data from Pilot Network Stations in Western Montana (2018–2022) and a Vision Forward

Camela Carstarphen, Jacqueline Timmer, John I. LaFave, Chris Gammons, Kim Bolhuis, W. Payton Gardner, James Swierc, Kelsey Jencso, and Stephanie Ewing

Montana Bureau of Mines and Geology

Front photos: (Left) MacDonald Pass in winter 2020, with student Kory Riley. (Top right) Lolo Pass in summer, with Big Sky Watershed Corp member Lauren Herbine. (Bottom right) Lolo Pass snow pit, with Camela Carstarphen and Adam Muscarella (USFS).

Montana Precipitation Isotope Network (MTPIN): 4-Year Stable Water Isotope Data from Pilot Network Stations in Western Montana (2018–2022) and a Vision Forward

Camela Carstarphen, Jacqueline Timmer, John I. LaFave, Chris Gammons, Kim Bolhuis,

W. Payton Gardner, James Swierc, Kelsey Jencso, and Stephanie Ewing

Montana Bureau of Mines and Geology

Montana Bureau of Mines and Geology Ground-Water Open-File Report 25

2024

https://doi.org/10.59691/DLIU2572

TABLE OF CONTENTS

Abstract/Summary 1
Introduction 1
Background 1
Study Area 4
Climate 4
Purpose and Scope 4
Pilot Network Sites 4
Upper Clark Fork Basin 4
Upper Missouri Basin 5
Blackfoot Basin 5
Bitterroot Basin–Lolo Watershed 6
Methods 6
Sample Collection 6
Precipitation Sampling 6
Snowpack Sampling 8
Tritium Sampling 9
Climate Data 9
Analytical 9
Local Meteoric Water Line Calculation 11
Results 13
Upper Clark Fork Basin 13
Upper Missouri Basin 17
Blackfoot Basin 17
Bitterroot Basin–Lolo 17
Tritium 19
Summary and Discussion 22
Western Montana Meteoric Line 22
Comparison to Previous Work 23
Snowpack 25
Tritium 25
Sampling Lessons Learned 25
Sample Handling 25
Data Management 26
Looking Forward 26
Acknowledgments 27
References 27
Appendix A: Site Data 31
Appendix B: Site Schedule for Bottle and Delivery Mechanism Exchange 43
Appendix C: Tritium Values 45
Appendix D: Data Analysis Methods Used to Identify Errors 47
Appendix E: Graph of Site $\delta^{18}O$ Data by Basin 49

FIGURES

Figure 1. Map of Montana; eight pilot network sites with HUC eight watersheds 2
Figure 2. Schematic of Palmex Rain Sampler 1. 7
Figure 3. Winter sampling at Basin Creek SNOTEL and Lolo Pass SNOTEL. 8
Figure 4. Sample split data from three different labs. 11
Figure 5. (A) Boxplot of *d-excess* values for all sample results; outlier values start at -6.8‰ and end at -62.0‰. (B) Boxplot of *d-excess* values for the groomed and final dataset. 12
Figure 6. The Upper Clark Fork basin with site LMWLs. 14
Figure 7. Winter 2018–2019 snowpack data graphed with the basin LMWL and winter precipitation values. 15
Figure 8. Annual precipitation amounts 16
Figure 9. Boxplot of temperature at each site, grouped by basin. 16
Figure 10. The Upper Missouri basin with site LMWLs graphed above the combined basin LMWL graphed with GMWL. 18
Figure 11. Winter 2018–2019 snowpack data graphed with the basin LMWL and winter precipitation values. 19
Figure 12. Lubrecht–Jones Pond is the only Blackfoot basin site. 20
Figure 13. The Bitterroot–Lolo basin site LMWLs graphed together, and then below the combined basin LMWL graphed with GMWL and precipitation. 21
Figure 14. Winter 2018–-2019 snowpack data graphed with the basin LMWL and winter precipitation values. 22
Figure 15. Tritium values from all sites are plotted by collection month and year. 23
Figure 16. Tritium values plotted by season: spring–early summer (March–August) and fall–early winter (September–January). 23
Figure 17. Graph of all precipitation data used in analysis, plotted with the Western Montana LMWL by season. 24
Figure 18. Graph of previous LMWLs, including our Western Montana LMWL. 24
Figure 20. Map of current collection MTPIN long-term network sites, 2024. 26

TABLES

Table 1. Pilot network site variables and annual precipitation. 5
Table 2. Timetable of site collection and number of samples as of December 1, 2022. 7
Table 3. Snowpack measurement and sampling. 15
Table 4. Four-year averages of $\delta^{18}O$ ‰, *d-excess*‰ and temperature (°C). 15
Table 5. Montana Local Meteoric Water Lines. 24

ABSTRACT/SUMMARY

Oxygen-18 and deuterium were measured from precipitation samples collected at eight sites in four different basins located in Montana's western climate region. Samples were collected over 4 yr (November 2018–November 2022) as monthly composites using the International Atomic Energy Agency (IAEA) Global Network of Isotopes in Precipitation's (GNIP) designed and developed collector. Sample sites were located in the Upper Clark Fork, Upper Missouri, Lower Blackfoot, and Lower Bitterroot Basins. Sites were located at high and low elevations in three basins (Upper Clark, Upper Missouri, and Lower Bitterroot) and adjacent to either a Montana Climate Office climate station or a Natural Resources and Conservation Service (NRCS) SNOTEL site for climate variables. Monthly composite samples included snowpack during the first two winters (2018–2019 and 2019–2020) at three high-elevation sites. A total of 387 precipitation samples and 43 snowpack samples were analyzed for stable water isotopes by the Montana Bureau of Mines and Geology (MBMG) Analytical Laboratory. The data were used to create a Local Meteoric Water Line (LMWL) for each site using a precipitation-weighted method. The LMWLs for sites within a basin differed little (slopes varied by 0.04 to 0.17), and basin LMWL slopes were between 7.64 and 7.81. These similarities suggest a single LMWL for the western climate region: $\delta 2H = 7.75 (\pm 0.06) \delta 18O + 2.95 (\pm 1.17)$. No elevation lapse rate in δ18O‰ values was observed in any basin and the δ18O‰ ranged from a February winter low of -29.9‰ (February 2019, Upper Missouri Basin) to a summer high of -3.6‰ (August 2020, Upper Clark Fork Basin). Snowpack isotopic composition was lightest in February, in response to February's isotopic light precipitation and high contribution to snow depth. As snowpack mass depleted during mid-March to mid-April, the snowpack isotopic signature was observed to become heavier, but did not deviate from the LMWL. All original sites are included in the International Atomic Energy Agency's GNIP network. Data collection continues at three of the original sites (as of July 2024). Some monthly samples were also analyzed for tritium (34 precipitation samples and one snowpack core). The results showed a distinct difference between spring–summer samples (median = 10.3 TU) and fall–winter samples (median = 6.0 TU). Site information and stable water isotope analytical data can be accessed at the Montana Bureau of Mines and Geology's Groundwater Information Center portal: http///mbmggwic.mtech.edu.

INTRODUCTION

The Montana Bureau of Mines and Geology (MBMG) Groundwater Assessment Program (GWAP) began a pilot project to collect monthly composite precipitation samples at eight sites in four western Montana basins (fig. 1). This work was done to test the feasibility of establishing long-term precipitation monitoring sites and develop methods to collect monthly composite samples at locations that receive rain and snow over the course of the year. Sample collection was aided by collaborators in each basin from universities and local water-quality districts.

The samples were collected to document the composition of deuterium (^{2}H) and oxygen-18 (^{18}O) in precipitation and develop local meteoric water lines (LMWL). Periodically between October 2018 and May 2020, samples from four sites were also analyzed for tritium (^{3}H), the radioactive isotope of hydrogen. Two of those sites were chosen to continue analysis for a full year (September 2020 through August 2021). Sample collection began in 2018 and was completed in November of 2022; over the course of the project, 430 stable-isotope samples (387 precipitation, 43 composite snowpack) and 35 tritium samples were analyzed. Analysis of the stable-water isotopes was completed by the MBMG Analytical Laboratory. The first set of periodic tritium analyses were completed by the University of Waterloo Environmental Laboratory and the second set of monthly samples analyzed by the International Atomic Energy Agency's Isotope Hydrology Laboratory. Stable water isotope data are available online at MBMG's Groundwater Information Center (GWIC, www.mbmggwic.mtech.edu).

Background

Stable water isotopes in precipitation have been analyzed globally since the 1950s, initially in a joint effort by the International Atomic Energy Agency (IAEA) and the World Meteorological Organization (WMO). In 1961, IAEA established the Global Network of Isotopes in Precipitation (GNIP) to collect and manage isotope precipitation data; those data are available through an online portal, WISER (Water Isotope

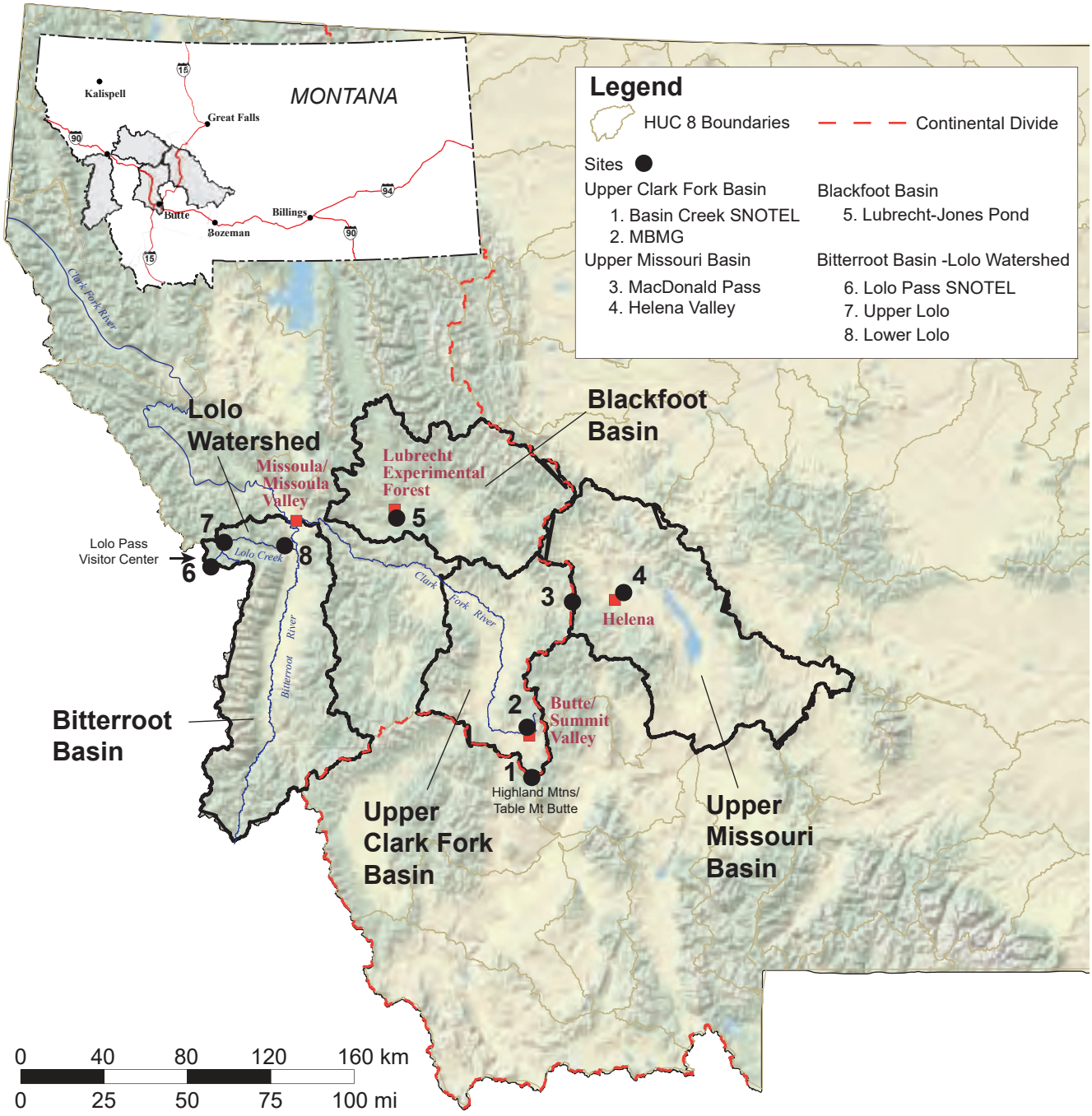

Figure 1. Map of Montana; eight pilot network sites with HUC eight watersheds.

System for Data Analysis, Visualization and Electronic Retrieval; https://nucleus.iaea.org/wiser). The GNIP website also provides guidelines for collection and data analysis.

Craig (1961), Dansgaard (1964), and more recently, Rozanski and others (1993), established the fundamental global relationship of hydrogen and oxygen isotopes in precipitation, including key principles driving isotope fractionation during evaporation, vapor transport and deposition, and standard analysis and reporting protocol (analyzing and reporting isotopic composition relative to the Vienna standard, VSMOW).

The ratio of the stable isotopes of hydrogen ($^{2}H/H$) and oxygen ($^{18}O/^{16}O$) reflects precipitation source and fractionation processes during travel and deposition; these phase changes affect the enrichment of one isotope relative to another and define the relationship of ^{18}O to ^{2}H at the site of deposition. Craig (1961) defined the global relationship (an average of all the GNIP site-specific data) between ^{18}O and ^{2}H in precipitation as $\delta^{2}H = 8 * \delta^{18}O + 10$. This Global Meteoric Water

Line (GMWL) describes the average covariant relation between the two isotopes, as a ratio normalized to the Vienna Standard Mean Oceanic Water (VSMOW). Rozanksi and others (1993), using a larger GNIP dataset, refined the GMWL to: $\delta^2H = 8.13*\delta^{18}O + 10.8$, and highlighted the spatial and temporal variation of ^2H and ^{18}O in precipitation. Their work highlighted that site-specific (local) isotopic composition in precipitation is controlled by temperature (season and elevation), latitude, and distance from the coast.

Because groundwater originates as precipitation, defining the local isotopic content and variation can be helpful to investigate groundwater recharge and flow. Local precipitation data can more precisely define the relationship between ^{18}O and ^2H that constitutes the recharge water for an area (e.g., Putnam and others, 2019), thereby providing necessary data to aid in local hydrologic study.

The use of stable water isotopes in hydrologic studies is well established; they have been used to interpret past climate (Dansgaard and others, 1993), atmospheric circulation (Dansgaard, 1964; Froehlich and others, 2002), water movement through watersheds (McDonnell and others, 1991; Steward and others, 1991), the provenance of stream flow (Sklash and Farvolden, 1979; Beisner, 2018), the location of groundwater recharge (Rye and Truesdell, 1993), residence time of streamflow and groundwater (McGuire and McDonnell, 2007; McDonnell and Klaus, 2015; Jasechko, 2019; Gardner and others, 2016), and the partitioning of water among plants, groundwater, and surface water (Evaristo and others, 2015). Key to these hydrologic studies is the use of local precipitation to calculate a local meteoric water line (LMWL) to understand annual, seasonal and topographic variation.

A meteoric water line derived from local precipitation data may differ from the GMWL. A measure of that variance is the value of *d-excess* defined by Dansgaard (1964) as $d = \delta^2H - 8 * \delta^{18}O$ (derived from Craig's GMWL equation). As precipitation forms, humidity and temperature affect the relative proportions of ^{18}O and ^2H. Local conditions may be different than the global average; consequently, the local values for *d-excess* shift away from the global average.

Low-humidity areas like Montana (with correspondingly low vapor pressure) can experience non-equilibrium processes in both summer and winter (Putnam and others, 2019). In summer, warm conditions and low humidity will produce sub-cloud evaporation as rain falls, producing negative *d-excess* values (Froehlich, 2002). In winter, during snow formation, mid-latitude areas often experience multiple phase changes between vapor and solid within the cloud (mixed cloud phase conditions), which result in non-equilibrium fractionation, resulting in a higher *d-excess* value. These two seasonal processes will affect both the slope and the y-intercept of the LMWL. Although the GMWL is a useful general framework for surface and groundwater studies, LMWLs provide a more precise framework for comparing and interpreting data from groundwater and surface waters (Coplen and others, 2000; Putnam and others, 2019).

Few LMWLs have been developed for Montana, and those that are available for western and southwestern Montana have used a variety of sample types (stream, precipitation, and/or snow core). Kendall and Coplen (2001) used USGS stream data; Kharka and others (2002) and Benjamin and others (2004) used snow core and summer precipitation. Gammons and others (2006) developed the first precipitation-based (12-mo event collection) LMWL. These past LMWLs are discussed in a later section.

Developing a robust LMWL is a multi-year effort; monthly-composite sampling over a 48-mo period is recommended to capture seasonal and annual variations (Wang and others, 2018; Putnam and others, 2019). Because western Montana experiences a strong seasonal precipitation gradient, with most occurring in the winter as snowpack, characterizing the seasonal variations and isotopic changes in the winter snowpack can be useful to investigate groundwater recharge.

An additional water isotope, tritium (^3H), can be used to understand groundwater residence and help define watershed hydrology. This radioactive isotope of hydrogen, with a half-life of 12.32 yr, is produced naturally in the upper atmosphere. However, aboveground testing of nuclear weapons between 1952 and 1963 injected large amounts of tritium into the atmosphere, overwhelming the natural production. Tritium concentrations in North American rainfall are estimated to have been in the range of 3 to 6 tritium units (TU) prior to nuclear testing. During the early 1960s, tritium concentrations in precipitation of more than 5,000 TU were recorded at several North American

stations (Solomon and Cook, 2000). Since then, most of the bomb-derived tritium has been washed from the atmosphere, and tritium levels in precipitation are now presumed to be close to natural levels (Clark and Fritz, 1997). Because of its short half-life, tritium is an ideal marker of recent (post-1952) groundwater recharge.

Although commonly used in groundwater studies, few Montana precipitation samples have been analyzed for tritium. Tritium deposition across the United States has been estimated from USGS and GNIP data (Michel and others, 2018; Lindsey and others, 2019). Samples from stations on the east coast suggest that annual precipitation varies between 3 and 14 TU (Michel and others, 2018).

Study Area

Precipitation samples were collected from four watersheds in western Montana: Upper Clark Fork, Upper Missouri, Lower Blackfoot, and Lower Bitterroot–Lolo (fig. 1). All the watersheds are located within the Northern Rocky Mountain Intermontane Basins physiographic province, which is characterized by generally north-trending mountain ranges separated by valleys (intermontane basins). The valleys (basins) contain through-flowing drainages and are typically flanked by floodplains and alluvial terraces. The "basins" are topographic and geologic features that are structurally downdropped relative to the surrounding mountains and are filled with unconsolidated to poorly consolidated Cenozoic deposits (Kendy and Tresh, 1996). Elevations across the four basins range between 3,116 m (10,223 ft) at Table Mountain south of Butte, Montana and 978 m (3,209 ft) in Missoula Valley, Missoula, Montana. The Continental Divide separates the Upper Clark Fork and Upper Missouri watersheds (fig. 1).

Climate

The climate is characterized by cold, snowy winters and mild summers. Most precipitation in the region is derived from moisture-rich Pacific air, although the region is affected by Arctic and Gulf of Mexico moisture sources at different times of the year, such as summer storms that originate from southwest monsoonal events (Whitlock and others, 2017). The higher-elevation mountainous regions receive heavy winter snowpack that is a significant source of water to valley bottoms and groundwater recharge. Many valley bottoms receive less than 300 mm (12 in) of moisture annually, whereas adjacent mountain ranges may receive more than 1,500 mm (60 in) of annual precipitation. Historical trends show the region becoming slightly warmer and drier; between 1950 and 2015, the average annual temperature increased by 0.4° F/decade while average annual precipitation decreased by 15 mm/decade (Whitlock and others, 2017).

Purpose and Scope

The purpose of this study was to develop a network of monthly precipitation sampling sites across a range of elevations in four western Montana basins to characterize the isotopic content. The specific objectives were to: (1) establish a network of precipitation collection sites and recruit local collaborators to assist with monthly sample collection, (2) develop a standardized sampling protocol for rain and snow sites and to compare different sampling techniques for winter snow sites, (3) use the data to determine unique LMWLs, and (4) characterize the range of tritium concentrations in precipitation.

Pilot Network Sites

The sample-collection sites are located in four basins in western Montana (fig. 1): Upper Clark Fork (two sites), Upper Missouri (two sites), Blackfoot (one site), and Bitterroot–Lolo watershed (three sites). Five sites are west of the Continental Divide (MBMG, Lubrecht-Jones Pond, Lolo Pass SNOTEL, Upper Lolo, and Lower Lolo), two are located on the Continental Divide (Basin Creek SNOTEL and MacDonald Pass), and one is just east of the Continental Divide in the Helena Valley (Helena Valley). To assess elevation effects, and any change in isotopic composition with elevation (a lapse rate), low- and high-elevation sites were established in each basin (except the Blackfoot; table 1). A unique identifier (GWIC ID) was established for each site (appendix A). Sites were adjacent to either a Montana Climate Office climate station or a NRCS SNOTEL site for climate variables (the exception is the Helena Valley site, which was located near a NOAA weather station).

Upper Clark Fork Basin

The Upper Clark Fork basin sites are located in the Summit Valley, near the city of Butte, Montana along the Continental Divide (fig. 1). The low-elevation site, located adjacent to the Montana Bureau of Mines and Geology building (MBMG, 1,762 m; table 1), is

Table 1. Pilot network site variables and annual precipitation.

Pilot Network Sites by Basin	GWIC No.	GNIP No.	Latitude	Longitude	Elevation (m)	Elevation (ft)	Annual Precipitation 4-yr Average (mm)[2]
Upper Clark Fork							
Montana Tech Campus	297504	7277401	46.01378	-112.5614	1762	5781	333
Basin Creek SNOTEL	298870	7277402	45.79718	-112.5205	2170	7119	498
Winter bucket[1]	304014	7277402	45.79718	-112.5205	2170		
Upper Missouri							
Helena Valley (USGS)	298826	7277200	46.61218	-111.9878	1160	3806	274
MacDonald Pass	298420	7277201	46.56434	-112.3076	1935	6348	624
Winter bucket[1]	304011	7277201	46.56434	-112.3076	1935		
Lower Blackfoot							
Lubrecht–Jones Pond	297503	7277301	46.89453	-113.4377	1231	4039	506
Winter bucket[1]	304014	7277301	46.89453	-113.4377	1231		
Lower Bitterrooot–Lolo							
Lower Lolo[3]	292006	7277302	46.748241	-114.1339	998	3275	487
Upper Lolo[3]	292026	7277303	46.74652	-114.5164	1241	4072	550
Lolo Pass SNOTEL	304000	7277304	46.63478	-114.5814	1673	5489	1170
Winter bucket[1]	304005	7277304	46.63478	-114.5814	1673		

[1]Winter collection augmented by second method: 5-gallon HDPE bucket in winter months at high-elevation sites.

[2]All monthly composite data in appendix A.

[3]2-yr average.

paired with a Montana Climate Office (MCO) climate station (https://www.umt.edu/climate), and the high-elevation site is adjacent to the Basin Creek SNOTEL site (2,170 m; table 1). The elevation difference between the sites is 408 m; both sites are in the upper Clark Fork River headwaters region (Columbia River Basin).

The MBMG site is on an open grassland slope on the northwest edge of town. The Basin Creek SNOTEL site is within the Deer Lodge–Beaverhead National Forest and on the slopes of the Highland Mountains 20 km (12 mi) to the south.

Upper Missouri Basin

The Upper Missouri Basin sites are located in the Helena Valley near Helena, Montana. The low-elevation site is on the east side of the Helena Valley (1,160 m; table 1, fig. 1, Helena Valley). This is the only site located east of the Continental Divide; it is adjacent to the National Oceanic and Atmospheric Administration climate station at the Helena airport. The high-elevation site is located on the Continental Divide at MacDonald Pass (1,935 m; table 1); it is paired with an MCO climate station.

The Helena Valley site is in open grassland on the east side of airport grounds, 25 km (16 mi) to the east of MacDonald Pass. The MacDonald Pass site is located in the Lewis and Clark National Forest where the Continental Divide crosses US Highway 12. The site is in a lightly forested area with mixed open grassland. Drainage to the east is into the upper Missouri headwaters region, which becomes the Mississippi River Basin, and to the west drains into the upper Blackfoot River headwaters, which drains into the Columbia River Basin.

Blackfoot Basin

The only site in the Blackfoot Basin is located at the Lubrecht–Jones Pond (1,231 m; table 1) in the University of Montana's Lubrecht Experimental Forest, 48 km (30 mi) northeast of Missoula, Montana

(fig. 1). The site is located in the lower part of the Blackfoot Basin, on a tributary to the Clark Fork River (Columbia River Basin). This site is paired with an MCO climate station in an open grassland area adjacent to forest.

Bitterroot Basin–Lolo Watershed

There are three sites located in the Lolo Creek watershed, a tributary to the Bitterroot River (fig. 1). The sites are located along the axis of Lolo Creek, over a distance of 45 km (29 mi). The high-elevation site is at the Lolo Pass SNOTEL station on the Idaho–Montana state line (1,673 m; table 1) near the Lolo Pass visitor center; it marks a transition zone between a wet Pacific northwest ecosystem and a Rocky Mountain subalpine woodland. The Upper Lolo site (1,241 m; table 1) marks a point where the valley slope decreases from steeper headwaters that are part of Lolo Creek. The Lower Lolo site (998 m; table 1) is on the edge of a small clearing upgradient of the confluence with the Bitterroot River (Columbia River Basin).

Lolo Pass is marked by heavy, wet snowfall with an annual average of 1,170 mm (46 in), twice that of the other two high-elevation sites (Basin Creek SNOTEL and MacDonald Pass; table 1). Precipitation averages decreased sharply between the SNOTEL and other sites; the Upper Lolo site recorded an average of 550 mm (22 in), similar to Lower Lolo at 487 mm (19 in). Of the three sites, the Upper Lolo site recorded the lowest average monthly temperature (-10°C, February 2019) and Lower Lolo the highest average monthly temperature (19°C, August 2020).

Sample collection from the upper and lower Lolo sites was discontinued after 2 yr because of the similarity in ^{18}O values (no significant elevation lapse rate) among all three sites, and the similarity in 2-yr LMWLs. The Lolo SNOTEL was kept as the only collection site and samples were collected for 4 yr.

METHODS

Sample Collection

Samples were collected as monthly precipitation (rain and snow) composites and analyzed for stable water isotope composition (δ^2H, $\delta^{18}O$). In addition, for the first 2 yr (2018–2020), winter and spring composite snowpack samples (from a complete core of the snowpack) were collected during the fall, winter, and spring monthly visits that snow was available (November through May) at the three high-elevation sites (Basin Creek SNOTEL, MacDonald Pass, and Lolo Pass SNOTEL); those visits included snowpack depth and SWE (snow-water equivalent) measurements. Between October 2018 and May 2020, tritium analyses were performed periodically on spring and fall samples collected at the Basin Creek SNOTEL, MacDonald Pass, Lubrecht–Jones Pond, and Lolo Pass SNOTEL sites (appendix A). From September 2020 through September 2021, monthly samples from the Basin Creek SNOTEL and Lolo Pass SNOTEL were analyzed for tritium as part of GNIP's global sampling program (appendix A).

Precipitation Sampling

The initial precipitation sampling sites were established in the Bitterroot–Lolo watershed in April 2018; the last site installation was at Basin Creek SNOTEL in October 2018. Table 2 lists start dates and the total number of samples collected and analyzed for each site; only samples collected between November 2018 through November 2022 are used and presented in appendix A. All stable water isotope data are available from the Ground Water Information Center (http:www.mbmggwic.edu).

Most of the precipitation samples were collected using a GNIP-designed precipitation collector (referred to as the collector) that is manufactured by Palmex (Gröning and others, 2012; IAEA, 2002; fig. 2). The collector is designed to isolate the samples from the atmosphere. A funnel captures precipitation and routes it through a tube to the bottom of the sample bottle, where it becomes submerged by the initial precipitation. The sample bottle is housed in an insulated cylinder that is fit with a pressure equilibrium tube. Samples obtained using the collector are comparable to other methods (e.g., oil collector, ball-in-funnel); however, low precipitation in warm months (inadequate sample volume to submerge the delivery tube) and persistent cold temperatures in the winter (freezing sample and plugging collector tubing) can inhibit the collector performance (Michelsen and others, 2018; Gröning and others, 2012). Collectors were installed at all sites following GNIP guidelines, and samples were collected between the last two days and first two days of each month (IAEA, 2014).

Table 2. Timetable of site collection and number of samples as December 1, 2022.

Pilot Network Sites by Basins	GWIC No.	GNIP No.	Latitude	Longitude	Start Date[1]	No. of samples
Upper Clark Fork						
MBMG	297504	7277401	46.01378	-112.5614	19 June 2018	56
Basin Creek SNOTEL	298870	7277402	45.79718	-112.5205	08 October 2018	53
Winter bucket	304014	7277402	45.79718	-112.5205	02 December 2018	20
Upper Missouri						
Helena Valley (USGS)	298826	7277200	46.61218	-111.9878	02 October 2018	49
MacDonald Pass	298420	7277201	46.56434	-112.3076	4 September 2018	51
Winter bucket	304011	7277201	46.56434	-112.3076	01 November 2018	21
Blackfoot						
Lubrecht–Jones Pond	297503	7277301	46.89453	-113.4377	08 June 2018	49
Winter bucket	304014	7277301	46.89453	-113.4377	01 February 2019	11
Bitterroot–Lolo Watershed						
Lower Lolo	292006	7277302	46.74824	-114.1339	15 March 2018	31[2]
Upper Lolo	292026	7277303	46.74652	-114.5164	7 June 2018	29[2]
Lolo Pass SNOTEL	304000	7277304	46.63478	-114.5814	7 June 2018	54
Winter bucket	304005	7277304	46.63478	-114.5814	29 November 2018	19

[1]Winter collection augmented at high-elevation sites with second method: 5-gallon HDPE bucket.
[2]Stations dropped after second year; data analysis showed little isotopic difference compared to Lolo Pass SNOTEL.

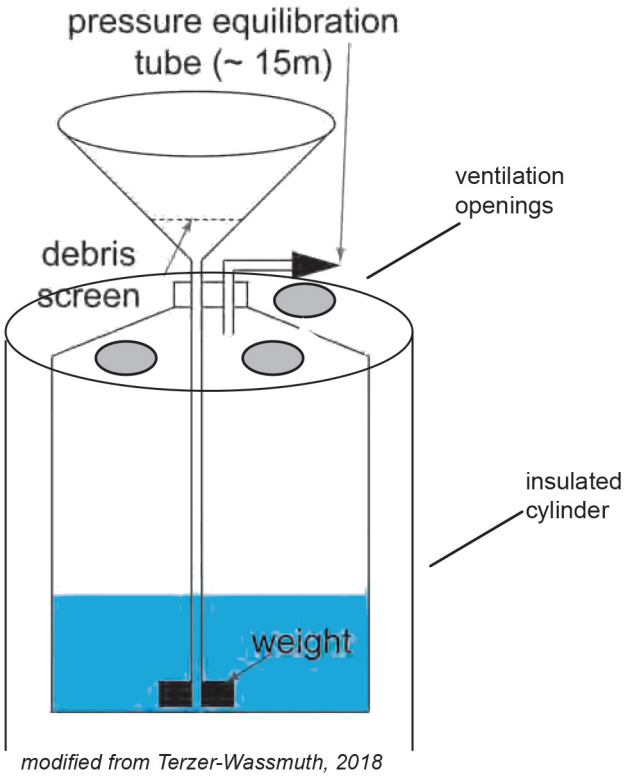

modified from Terzer-Wassmuth, 2018

Figure 2. Schematic of Palmex Rain Sampler 1. Bottle inserts from the bottom of the cylinder, screws in place, and is connected to the funnel by a narrow neck. A delivery tube or p-valve (siphon, used in winter) allows precipitation to move into bottle. Ventilation openings are at the top of the cylinder, which is insulated and wrapped with a pressure equilibration tube (entry shown on diagram, tube wraps within the cylinder housing from top to bottom). The tube helps to keep the bottle at atmospheric pressure. Samples are isolated from the atmosphere unless rain amounts are too small to properly submerge the delivery tube or if the siphon is left in when average daily temperatures are above 10°C (50°F).

The collector has two delivery tube options, a long narrow tube for warm months (daily temperature averages routinely above 10°C), and a small narrow plastic "snow siphon inlet" (Palmex item name) for sample collection during cooler months (daily average temperatures less than 10°C). The sample bottle has a 3-L volume. Because some months did not have adequate initial precipitation to submerge the delivery tube in the 3-L bottle, it was replaced with a 1.2-L bottle, which requires only 3 mm of precipitation to submerge the delivery tube. The smaller bottle has a capacity for 90 mm of precipitation, and so requires monitoring of precipitation amount if inadvertently deployed during a wet month (precipitation data available online). Although rarely necessary, there were a few instances when the bottles had to be switched out mid-month and totalized at the end. Bottles and delivery mechanisms were exchanged based on temperature and precipitation amounts; each site had its own schedule (appendix B).

Samples from the lower elevation sites (MBMG, Helena Valley, Lower Lolo, and Upper Lolo) were obtained exclusively from the collector. A 15-cm-diameter "snow tube" was placed over the collector's funnel during winter months (fig. 3). At the high-elevation sites (Basin Creek SNOTEL, MacDonald Pass, Lolo Pass SNOTEL) and the Lubrecht–Jones site, snow samples were collected using two methods: a HDPE 5-gal bucket and the collector (fig. 3).

Because of the large snow accumulation at the Lolo Pass SNOTEL site, multiple trips were required during winter months (December through March) to switch out the bucket sampler. At the end of the month, the total volume from the buckets was summed and mixed for a monthly precipitation sample. At Basin Creek SNOTEL and MacDonald Pass, a single bucket could be deployed for the entire month. Appendix A indicates the sample method used (collector/bucket). All samples were processed by filtering into a HDPE 20-ml bottle with no headspace and stored in a temperature-stable environment prior to lab analysis.

Snowpack Sampling

Monthly snowpack samples were taken at the three high-elevation sites during the first 2 yr (2018–2019 and 2019–2020) of the pilot effort. Samples were collected when there was adequate snow to use a federal snow sampler (November through May). The sample consisted of at least one complete snowpack core that was collected in a large HDPE bottle, capped, and allowed to slowly thaw before preparing for lab analysis. Samples were collected at the Lubrecht–

Basin Creek SNOTEL March 2019

Lolo Pass SNOTEL December 2018

Figure 3. Winter sampling at Basin Creek SNOTEL on the left and Lolo Pass SNOTEL on the right. Basin Creek SNOTEL is set up with the winter snow tube attached to sampler. The federal snow sampler kit used for snowpack measurement and collection into HDPE 3 liter bottles is open on the snow and the bottles are next to collector pole. Lolo Pass SNOTEL has snow tube and the 5-gal bucket attached to pole and secured in snow.

Jones Pond site when there was adequate snowpack; many months did not have sufficient snow accumulation (table 3). On each visit the ground conditions, ice incurred, and the overall ease or difficulty in obtaining a complete core were recorded. After the first 2 yr, snowpack sampling was reduced to once during accumulation (when the snowpack is increasing) and once during ablation (when the snowpack was rapidly losing volume through sublimation, compaction, and melt) when possible. Daily temperature, snow depth, and SWE data recorded at the SNOTEL sites were used to determine snowpack conditions.

The snowpack samples were collected to address questions such as:

- How does the isotopic content of the snowpack compare to the monthly snow-precipitation samples?
- Are there changes that occur isotopically in the snowpack over the course of the winter?
- Does the snowpack acquire an evaporative signature through ablation/sublimation?
- Can a properly timed snowpack sample adequately represent winter precipitation at a high-elevation site?

Tritium Sampling

Tritium analysis was conducted on precipitation samples collected from the high-elevation sites (Basin Creek SNOTEL, Lolo Pass SNOTEL, MacDonald Pass, and Lubrecht-Jones Pond). The initial analyses included samples from 2018 (fall), 2019 (spring and fall), and then 2020 (spring). Beginning in September 2020, monthly samples from the Lolo Pass SNOTEL and Basin Creek SNOTEL sites were collected for the IAEA GNIP global tritium project. All the tritium samples were stored in 500-mL HDPE bottles and held for less than a year. The samples collected between November 2018 and August 2020 were analyzed by the University of Waterloo's Environmental Isotope Lab (appendix A). Samples collected after September 2020 were analyzed at IAEA Isotope Hydrology Laboratory. A total of 35 monthly composite samples were analyzed; all sampled sites and data are included in appendix A, and tritium values in appendix C. Both laboratories report tritium concentration in tritium units (1 TU = 1 ^{3}H atom per $10^{18}H$ atoms).

Climate Data

Monthly precipitation totals were measured each month. Five sites (MBMG, MacDonald Pass, Lubrecht–Jones Pond, Lower Lolo, and Upper Lolo) were paired with a Montana Climate Office Mesonet Station (https://climate.umt.edu/mesonet). These stations provide temperature and vapor pressure data. Two sites, Basin Creek SNOTEL and Lolo Pass SNOTEL, have monthly average temperature data from the National Resources Conservation Service SNOTEL's data portal. A NOAA weather station close to the Helena Valley site was used for monthly average temperature and relative humidity. Climate data are presented in appendix A.

Analytical

Stable water isotope samples were analyzed at the MBMG Analytical Laboratory using a Picarro L2130-i Cavity Ring-Down Spectrometer (CRDS). The Picarro operating instructions were followed, including calibration frequency and methods. Each batch, or sample run, starts and finishes with a series of three known samples. All samples within the run are "corrected" using the line equations found for the "run curve."

Analytical results for ^{18}O and ^{2}H are reported as δ values, which represent the difference in parts per thousand (per mill, ‰) between the ratios of ^{18}O /^{16}O (or ^{2}H /^{1}H) to that of Vienna Standard Mean Ocean Water (VSMOW); δ values are determined by:

$$(\delta \text{ in } ‰) = (R_{sample}/R_{SMOW} - 1)*1{,}000,$$

where R is the ratio of the heavy to light isotope. Therefore, the results are interpreted relative to VSMOW. A positive δ value means that the sample contains more of the heavy isotope than standard ocean water; a negative δ value means that the sample contains less. Errors for $\delta^{2}H$ are <1‰ and <0.5‰ for $\delta^{18}O$.

Over the course of the study, split samples were sent to:

- The University of Waterloo Environmental Isotope Laboratory. This occurred twice over the course of the 4-yr effort and included samples from Lolo Pass SNOTEL (five samples, one snowpack), Lubrecht–Jones Pond (one sample), MacDonald Pass (four samples), and Basin Creek (three samples);

Table 3. Snowpack measurement and sampling.

	Date of Visit	Average SNOW Depth (cm)	Average Core Length (cm)	Average SWE* (cm)	$\delta^{18}O$ ‰	$\delta^{2}H$ ‰	Tritium (TU)
Upper Clark Fork Basin							
Basin Creek SNOTEL	1/2/19	33	31	7	-19.8	-152	
	1/30/19	51	45	11	-20.6	-155	
	3/6/19	85	91	17	-23.6	-181	
	3/31/19	76	55	17	-24	-183	
	5/1/19	42	36	16	-20.8	-160	
	1/2/20	40	35	9	-22	-165	
	2/1/20	43	36	10	-21.3	-161	
	2/27/20	61	55	14	-20.5	-155	
	4/2/20	74	41	9	-19.3	-147	
	4/28/20	NA	NA	NA	-19.6	-152	
	2/25/21	61	51	8	-22.7	-174	
	2/28/22	51	47	9	-24.1	-179	
Upper Missouri Basin							
MacDonald Pass	1/1/19	37	30	5	-18.5	-143	
	1/31/19	61	54	12	-19.4	-147	
	2/28/19	106	98	25	-24.6	-187	
	4/1/19	89	73	29	-23.1	-176	
	5/2/19	47	42	21	-20.9	-161	
	11/27/19	22	20	5.3	-17.5	-129	
	1/3/20	38	33	10	-20.3	-151	
	1/30/20	46	42	12.7	-19.9	-151	
	2/28/20	64	50	20	-19.6	-146	
	4/3/20	79	60	23	-19.4	-147	
	3/2/21	84	73	24	-20.4	-154	
	2/25/22	63	55	15	-23.2	-171	
Bitterroot–Lolo Watershed							
Lolo Pass SNOTEL	12/31/18	132	110	32	-16.9	-124	
	2/2/19	133	125	41	-17.8	-131	
	3/3/19	197	183	59	-20.6	-154	
	3/30/19	164	60	65	-20.3	-152	5.2
	4/30/19	131	129	64	-18.3	-139	
	5/14/19	65	64	33	-17.6	-131	
	12/2/19	23	20	2.2	-15.3	-108	
	1/4/20	97	74	18	-15.2	-109	
	1/31/20	149	134	38	-17.2	-124	
	2/29/20	185	165	55	-16.8	-123	
	4/4/20	188	167	53	-16.9	-124	
	5/2/20	108	100	52	-14.7	-109	
	2/26/21	205	183	58	-17.6	-132	
	4/30/21	88	88	44	-16.7	-124	
	3/2/22	131	118	47	-19.5	-143	
	4/15/22	149	126	55	-19	-141	
Blackfoot Basin							
Lubrecht–Jones Pond	2/1/19	45	30	8	-19.2	-154	
	3/1/19	80	52	15	-26	-200	
	3/29/19	37	23	13	-23.1	-178	

- University of Utah SIRFER Laboratory. In 2021, samples included Lolo Pass SNOTEL (six samples, two snowpack samples), Lubrecht–Jones Pond (five samples), MacDonald Pass (six samples, two snowpack samples), Helena Valley (five samples), Basin Creek SNOTEL (six samples, one snowpack sample), and MBMG (five samples); and
- IAEA Isotope Hydrology Laboratory. From August 2020 through August 2021, samples were submitted from Basin Creek SNOTEL (11 samples) and Lolo Pass SNOTEL (11 samples)

There were 75 split samples (19% of total). No single sample was sent to more than one other lab. The University of Utah's SIRFER Laboratory and the IAEA Isotope Hydrology Laboratory used a Picarro CRDS instrument; Waterloo used a Los Gatos Research (LGR) Liquid Water Isotope Analyser (LWIA). There was good agreement between the results from outside labs and the MBMG analytical lab (fig. 4). A plot of δ^2H results from the three labs against MBMG results in a linear regression line with an r^2 value of 0.99. A plot of $\delta^{18}O$ data has a linear regression line with an r^2 value of 0.94.

Local Meteoric Water Line Calculation

A local meteoric water line defines the relationship between δ^2H and $\delta^{18}O$ for precipitation falling in a region. The development of a robust and accurate LMWL typically requires data to be collected over 48 mo (Wang and others, 2018; Putnam and others, 2019). Many LMWLs have been calculated using regression techniques that give equal weighting to all data points regardless of the precipitation amount they represent (e.g., Gammons and others, 2006). In this study, local meteoric lines were calculated using the Hughes and Crawford (2012) precipitation-weighted, least squares regression protocol, using November 2018 through November 2022 data. A spreadsheet-based calculator developed by GNIP was used to perform the calculations.

The *d-excess* value was calculated for each sample and used to identify samples that may have been compromised by post-deposition evaporation. Worldwide, the *d-excess* values range from about -2 to 15 per mill (Froehlich, 2002); northern hemisphere values tend to be largest in the winter and smallest in the summer (Kreutz and others, 2003). However, in warm, arid climates, sub-cloud evaporation can result in low *d-excess* values as low as -16.3‰ (Crawford and others, 2017).

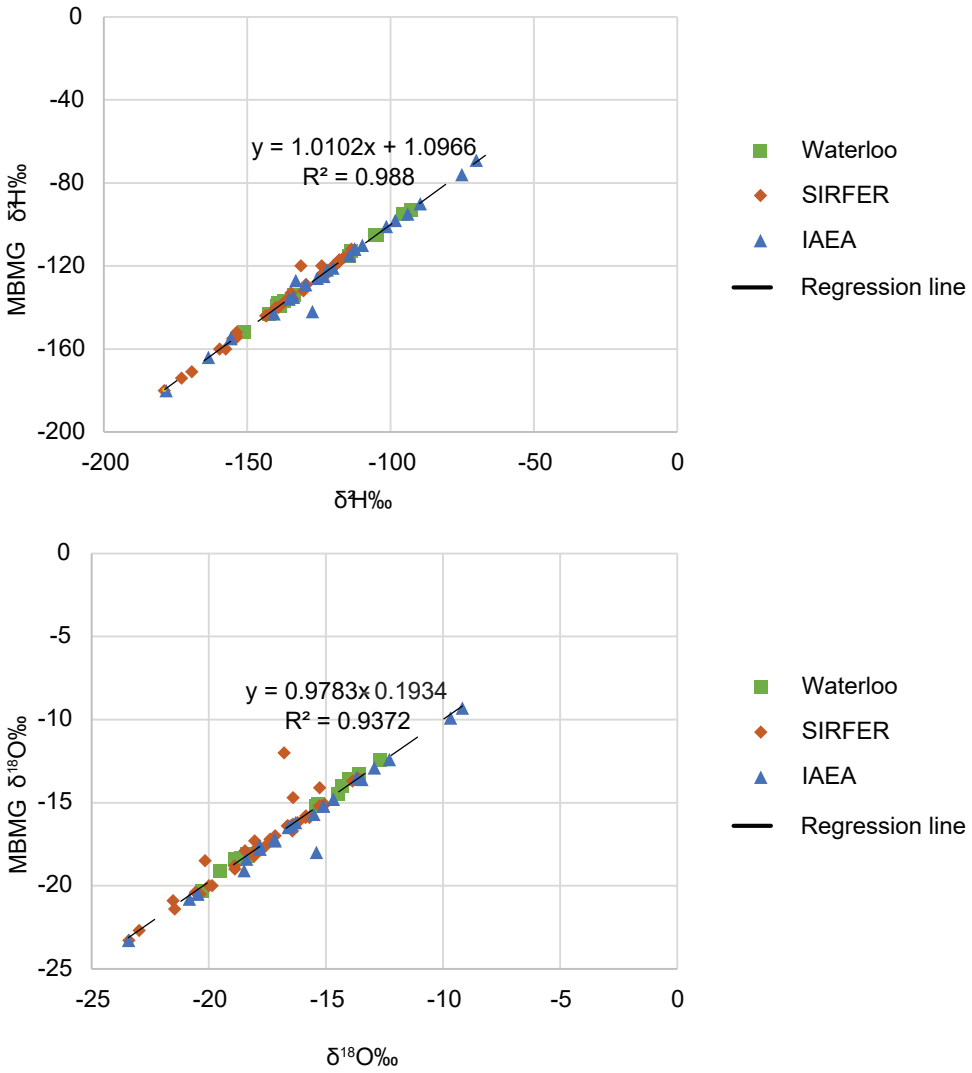

Figure 4. Sample split data from three different labs: University of Waterloo Environmental Laboratory (Waterloo), University of Utah SIRFER Laboratory (SIRFER), and International Atomic Energy Agency Laboratory (IAEA) are plotted together against the MBMG Analytical Laboratory results.

For this study, it was anticipated that low-precipitation summer events that did not submerge the collector delivery tube, as well as freezing conditions in the winter that blocked the delivery tube, may cause post-deposition evaporation/sublimation resulting in unrepresentative samples with anomalous *d-excess* values.

The *d-excess* values for all samples analyzed ranged from 16‰ to -62‰; the median was 5.8 (fig. 5A). Outlier values begin at -6.8‰ and do not mean that the sample collection or analysis has been compromised. To help refine a set of possible comprised data, a linear regression plot with the 95% confidence interval and a residual graph of that data, and a weighted bootstrap graph with confidence interval, were used (appendix D). This set was followed up with a review of precipitation daily amounts and field note analysis. This effort removed 25 samples that

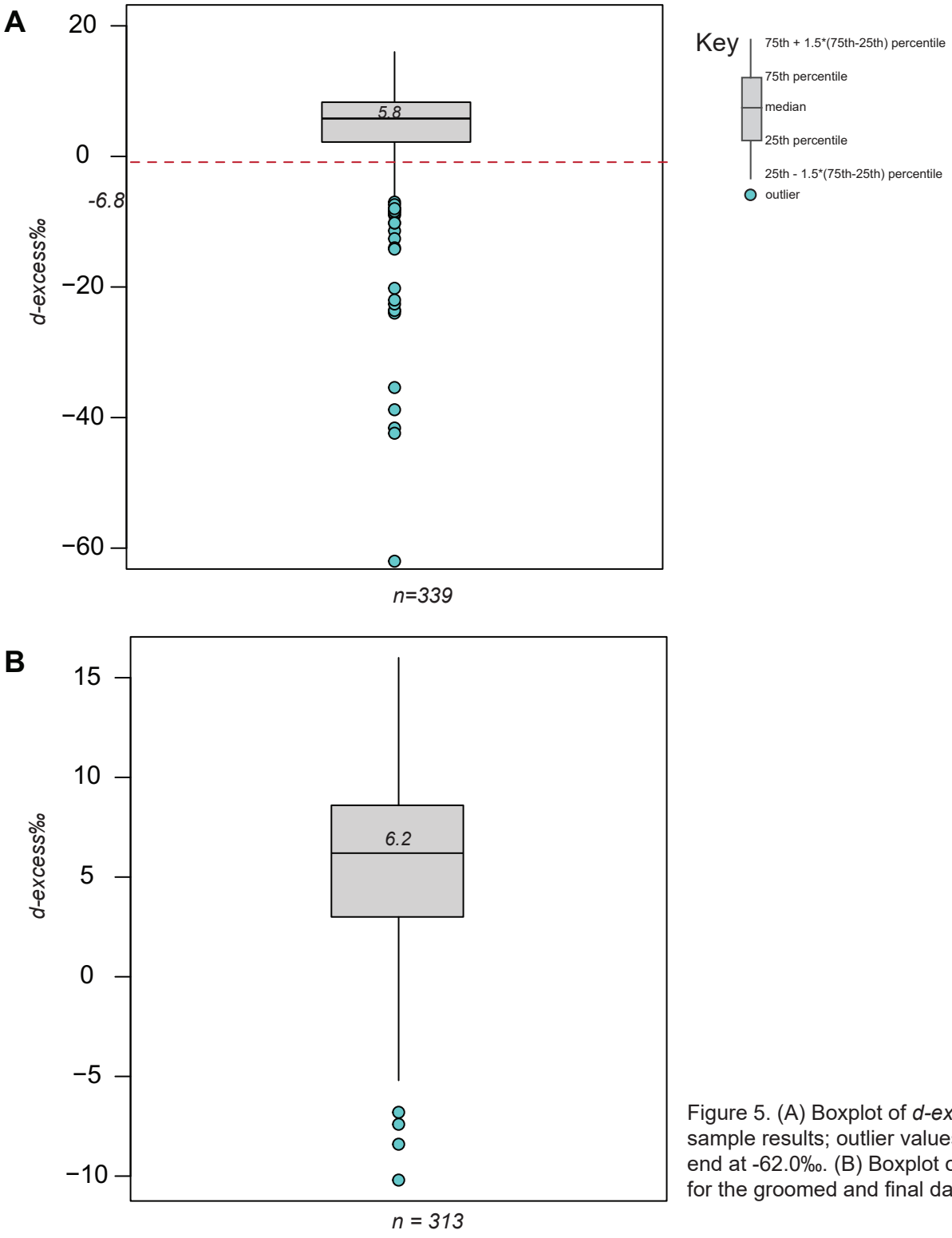

Figure 5. (A) Boxplot of *d-excess* values for all sample results; outlier values start at -6.8‰ and end at -62.0‰. (B) Boxplot of *d-excess* values for the groomed and final dataset.

were considered unrepresentative outliers (outlier values are from -7.0‰ to -62.0‰); a total of 313 samples was kept for LMWL computation. The final dataset *d-excess* values ranged from 16‰ to -10.2‰; outlier values start at -6.8‰ (fig. 5B). All data are presented in appendix A with excluded data noted.

At the high-elevation sites that used both a collector and a bucket in winter, only one value was used. In most cases the analytical results were similar, but during the shoulder season months (November and March) the bucket was sensitive to warm temperatures and the collector yielded better results. However, during the winter months (December, January, and February), conditions of snowfall and temperature variations sometimes created sublimation of the sample caught in the funnel. Field notes were used to choose the best sample result for those months. After 2 yr, only the bucket was used for December, January, and February.

RESULTS

The LMWL for each site and basin were calculated using a GNIP-developed Excel calculator based on a precipitation-weighted least squares regression method (Hughes and Crawford, 2012). Time-series plots of $\delta^{18}O$ values for all basins are represented in appendix E.

Upper Clark Fork Basin

The LMWLs for the Basin Creek SNOTEL (elevation 2,170 m) and MBMG (elevation 1,762 m) are similar despite the elevation difference (fig. 6).

Basin Creek SNOTEL:

$$\delta^2H = 7.80\ (\pm\ 0.11)\ \delta^{18}O + 3.98\ (\pm\ 2.04)\ [n = 48\ samples].$$

MBMG:

$$\delta^2H = 7.90\ (\pm\ 0.13)\ \delta^{18}O + 3.46\ (\pm\ 2.24)\ [n = 47\ samples].$$

There was no apparent elevation effect; differences in average $\delta^{18}O$ values between sites is 0.5‰ (table 4). There appears to be some variation at seasonal transition months (March, July, and November).

Because the results were similar, data from both sites were combined to develop a LMWL for the basin:

Upper Clark Fork Basin:

$$\delta^2H = 7.81\ (\pm\ 0.09)\ \delta^{18}O + 3.32\ (\pm\ 1.57).$$

The results from the 2018–2019 monthly composite snowpack samples from the Basin Creek SNOTEL site plot on the LMWL (fig. 7). December and January precipitation values are very similar, producing a snowpack composition of similar value. In general, the February precipitation was the lightest on record, in cases by as much as 9‰, and it usually marks a time of snowpack accumulation; this shifts overall snowpack composition to a lighter signature (fig. 7). March marks a transition in precipitation composition towards heavier values. The 2019 March precipitation (fig. 7) is similar in isotopic composition to the previous December and January. However, the March snowfall amount was not enough to alter, significantly, the overall snowpack (isotopic) composition (red square, fig. 7). Despite the heavier composition of March snowfall relative to February, the snowpack isotopic signature is impacted more by the isotopically light February snow contribution than March snowfall. This has significance for the isotopic signature of recharge melt during March ablation when snowpack loses mass and thickness (table 3). By April the snowpack has decreased in thickness by 45 percent (table 3) and the isotopic signature has become heavier, but still on the LMWL (fig. 7).

Over the sample period, precipitation averaged 333 mm/yr (13 in) at MBMG, and 497 mm/yr (20 in) at Basin Creek SNOTEL (appendix A, table 1). Peak precipitation occurred as snow (usually in January/February), and rain and snow from March through May. Although the annual precipitation at MBMG is less than at Basin Creek SNOTEL, both 2019 and 2020 were high-precipitation years for Basin Creek SNOTEL (MBMG showed less fluctuation; fig. 8). The temperature range at Basin Creek SNOTEL was less than at MBMG (fig. 9), but winter inversions in the valley produced warmer temperatures at higher elevations (appendix A). The monthly minimum temperatures varied between -12°C and -4°C, with the lowest temperatures recorded at the Basin Creek SNOTEL site (February 2019, appendix A). Maximum monthly temperatures varied between 14°C and 22°C, with the warmer monthly temperatures occurring at the MBMG site.

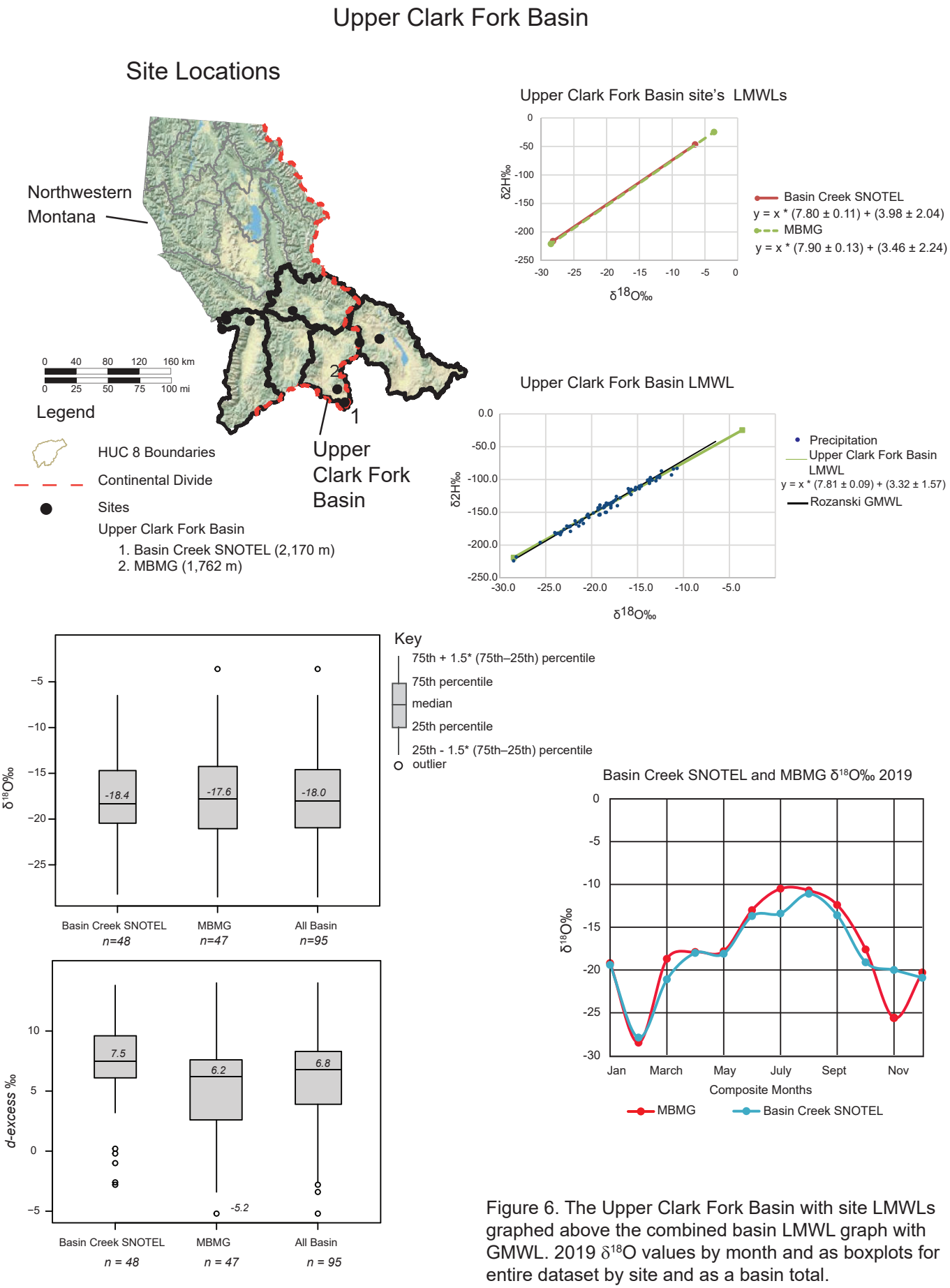

Figure 6. The Upper Clark Fork Basin with site LMWLs graphed above the combined basin LMWL graph with GMWL. 2019 $\delta^{18}O$ values by month and as boxplots for entire dataset by site and as a basin total.

Table 4. Four-year averages of $\delta^{18}O$ ‰, *d-excess* ‰, and temperature (°C).

Sites	$\delta^{18}O$‰	*d-excess* ‰	No. of Samples (*n*)	Site elevation (m)	T°C	No. of Samples (*n*)	*d-excess* Lapse Rate/100 m ‰
Upper Clark Fork							0.60
Basin Creek SNOTEL	-17.7	7.3	48	2,170	3.5	49	
MBMG	-17.2	4.9	47	1,762	4.9	49	
Difference	0.5	2.4		408			
Upper Missouri							0.32
MacDonald Pass	-17.7	6.8	45	1,935	3.1	48	
Helena Valley	-17.2	4.3	44	1,160	6.9	49	
Difference	0.5	2.5		775			
Blackfoot							
Lubrecht–Jones Pond	-16.6	4.9	41	1,231	4.5	49	
Bitterrroot–Lolo							
Lolo Pass SNOTEL	-15.9	7.4	44	1,673	4.1	49	
Upper Lolo	-15.8	4.8	23	1,241	3.6	24	0.60
Lower Lolo	-15.9	3.9	21	998	6.3	24	0.52
Difference							
Lolo Pass SNOTEL/Upper Lolo	0.1	2.6		432			
Lolo Pass SNOTEL/Lower Lolo	0.0	3.5		675			

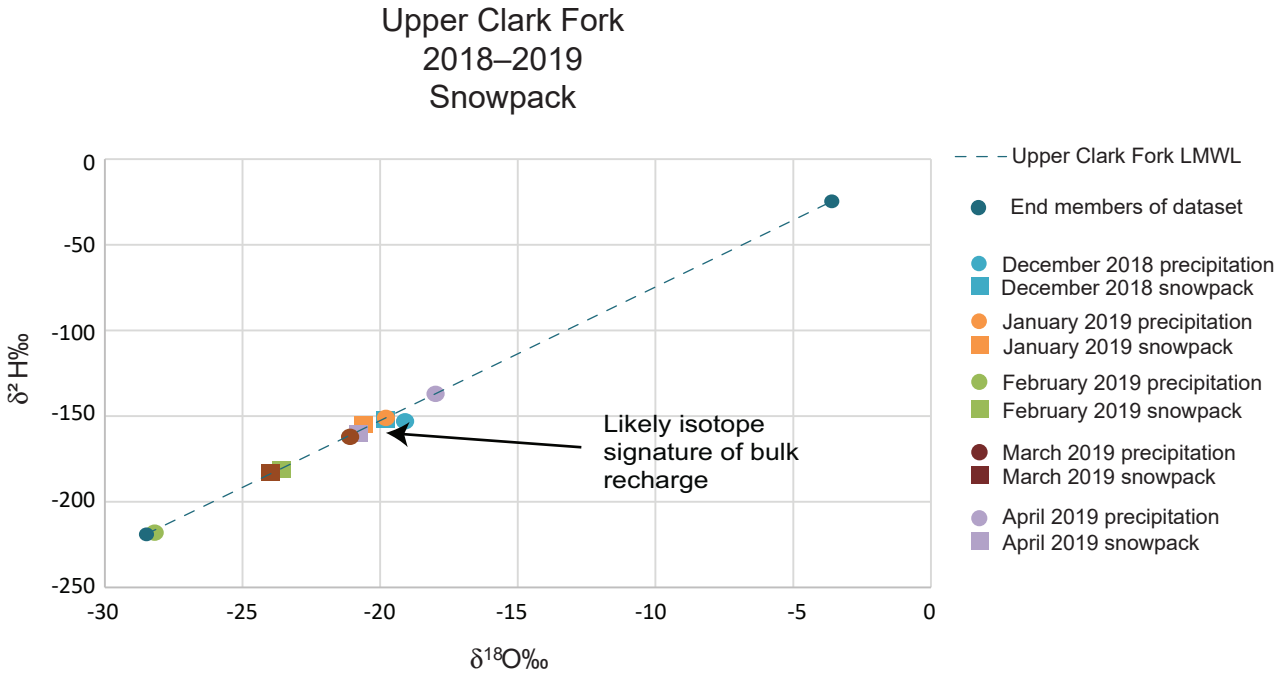

Figure 7. Winter 2018–2019 snowpack data graphed with the basin LMWL and winter precipitation values. The LMWL is marked with the dataset's lightest (winter) and heaviest (summer) end members.

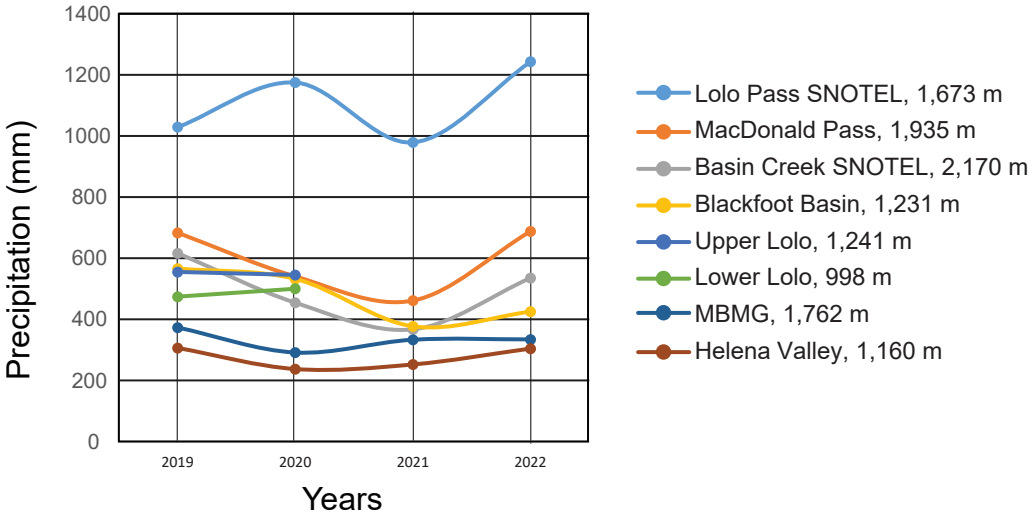

Figure 8. Annual precipitation amounts, Lolo Pass SNOTEL shown in blue.

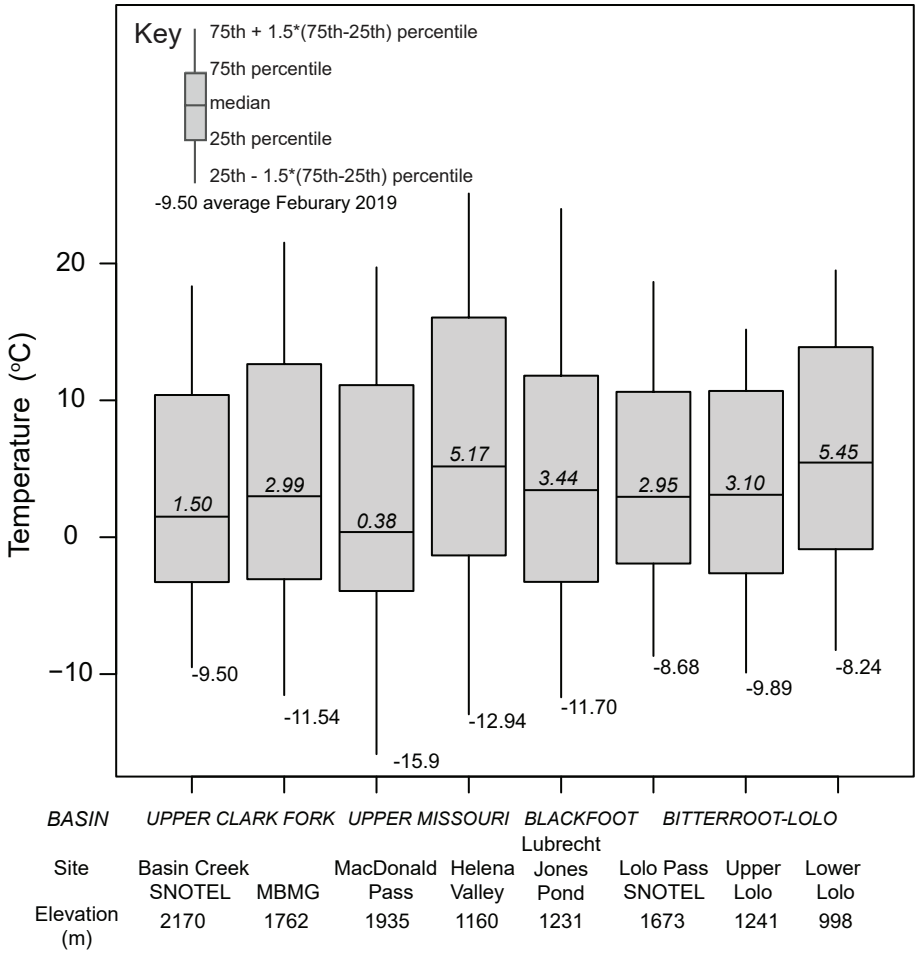

Figure 9. Boxplot of temperature at each site, grouped by basin. Medians are shown with values. February 2019 recorded the lowest monthly average for the 4 yr of data at every site, labeled on the graph.

Upper Missouri Basin

The LMWL regressions for the MacDonald Pass (1,935 m) and Helena Valley (1,160 m) sites are similar:

MacDonald Pass:

$\delta^2H = 7.72\ (\pm 0.15)\ \delta^{18}O + 2.61\ (\pm 2.88)$ [*n = 45 samples*].

Helena Valley:

$\delta^2H = 7.89\ (\pm 0.16)\ \delta^{18}O + 3.72\ (\pm 2.72)$ [*n = 44 samples*].

There is little difference in the seasonal variation of $\delta^{18}O$ values between the sites (fig. 10); therefore, the data from both sites were combined to calculate a single LMWL for the basin:

Upper Missouri Basin:

$$\delta^2H = 7.72\ (\pm 0.11)\ \delta^{18}O + 2.06\ (\pm 1.97).$$

The 2018–2019 MacDonald Pass composite snowpack samples plot on the LMWL (fig. 11). Snowpack data starts with December, but the snowpack is a composite of November and December snow. The 2018 November precipitation amount was greater than December; consequently, the November isotopic signature drives the total snowpack composition measured at the end of December. The February precipitation was isotopically the lightest of winter and greatest amount of snowfall (fig. 11); the snowpack increased in February (from an average depth of 61 cm (24 in) to 106 cm (42 in; table 3). This addition of isotopically lighter snow noticeably impacted the overall snowpack signature (fig. 11). At this site, changes in snowpack (drop in depth and increase in SWE) occurred quickly, moving the snowpack into ablation (table 3). This process of condensing, melting, and sublimating continues through April, producing an isotopically heavier snowpack than the winter accumulation, defining the likely bulk signature of recharge (fig. 11).

Over the sample period, annual precipitation averaged 624 mm/yr (25 in) at MacDonald Pass, and 274 mm/yr (11 in) at the Helena Valley site (appendix A, table 1). Three peak precipitation periods occurred; late winter snow, early summer rain, and mid-fall rain/snow. Helena Valley recorded the least annual precipitation of all sites (fig. 8). The temperature range was similar between the two sites (fig. 9); winter inversions caused some monthly temperature averages to be lower in the valley (appendix A). The monthly minimum temperatures varied between -15°C and -2°C (the coldest recorded at MacDonald Pass in February 2019); maximum monthly averages varied between 15°C and 25°C (Helena Valley, July 2021; appendix A).

Blackfoot Basin

The Lubrecht–Jones Pond site (1,231 m) is the only site in the lower Blackfoot Basin and is the northernmost of the four basins (fig. 12). The LMWL is similar to the others in the study:

Lubrecht–Jones Pond:

$$\delta^2H = 7.64\ (\pm 0.16)\ \delta^{18}O + 0.77\ (\pm 2.72)\ (n = 41).$$

The seasonal $\delta^{18}O$ values ranged from -23.5‰ to -9.7‰ (fig. 12) with an average of -16.6‰ (table 4). Precipitation amounts varied seasonally and annually (fig. 8); the highest and the lowest measured values occurred in July (2020, 125 mm and 2021, 5 mm; appendix A). Annual precipitation averaged 506 mm (20 in; table 1). Despite the very wet July in 2020, most precipitation occurred as snow in February and March, and as rain and snow in October. Minimum temperatures generally occurred in February and varied between -3°C and -12°C (appendix A). The warmest month was August 2022 (24°C; appendix A); the maximum monthly temperature averages varied between 17°C and 24°C. Similar to the other sites, February 2019 had the coldest temperature (-11.70°C; fig. 9).

Bitterroot Basin–Lolo

The LMWL regressions for the Lolo Pass SNOTEL (1,673 m), Upper Lolo (1,241 m), and Lower Lolo (998 m) sites are presented below and in figure 13:

Lower Lolo LMWL is:

$\delta^2H = 7.84\ (\pm 0.24)\ \delta^{18}O + 1.23\ (\pm 3.99)$ (*n = 21*).

Upper Lolo LMWL is:

$\delta^2H = 7.88\ (\pm 0.14)\ \delta^{18}O + 3.02\ (\pm 2.37)$ (*n = 23*).

Lolo Pass SNOTEL is:

$\delta^2H = 7.68\ (\pm 0.26)\ \delta^{18}O + 3.80\ (\pm 4.36)$ (*n = 44*).

Monthly $\delta^{18}O$ values were similar among the sites with no apparent lapse rate (fig. 13, table 4). There were differences in *d-excess* values: the average *d-excess* differed between Lolo Pass SNOTEL and the two lower sites; Lower and Upper Lolo sites differed

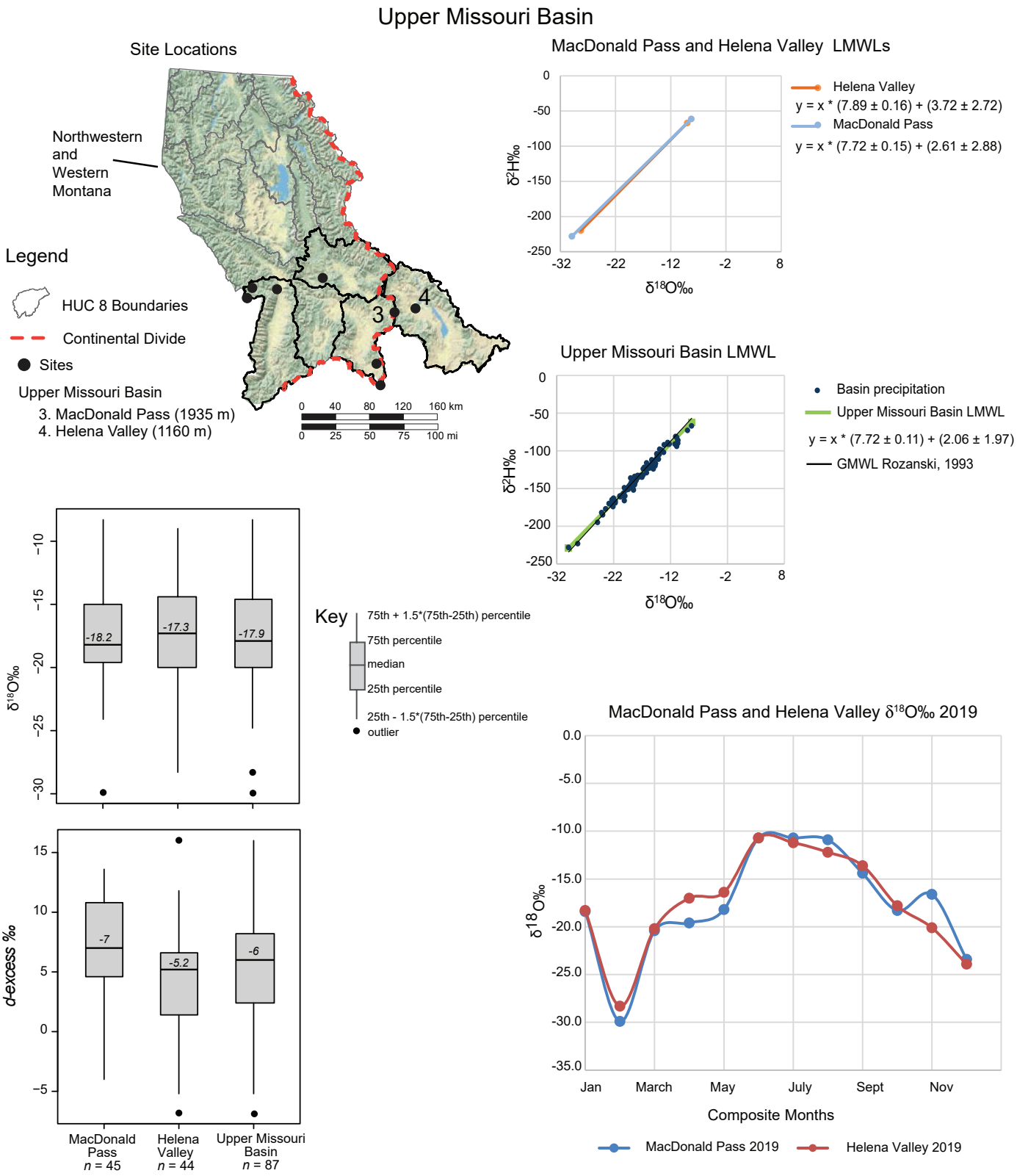

Figure 10. The Upper Missouri basin with site LMWLs graphed above the combined basin LMWL graphed with GMWL. 2019 $\delta^{18}O$ values are graphed by month and as boxplots by site and as a basin total.

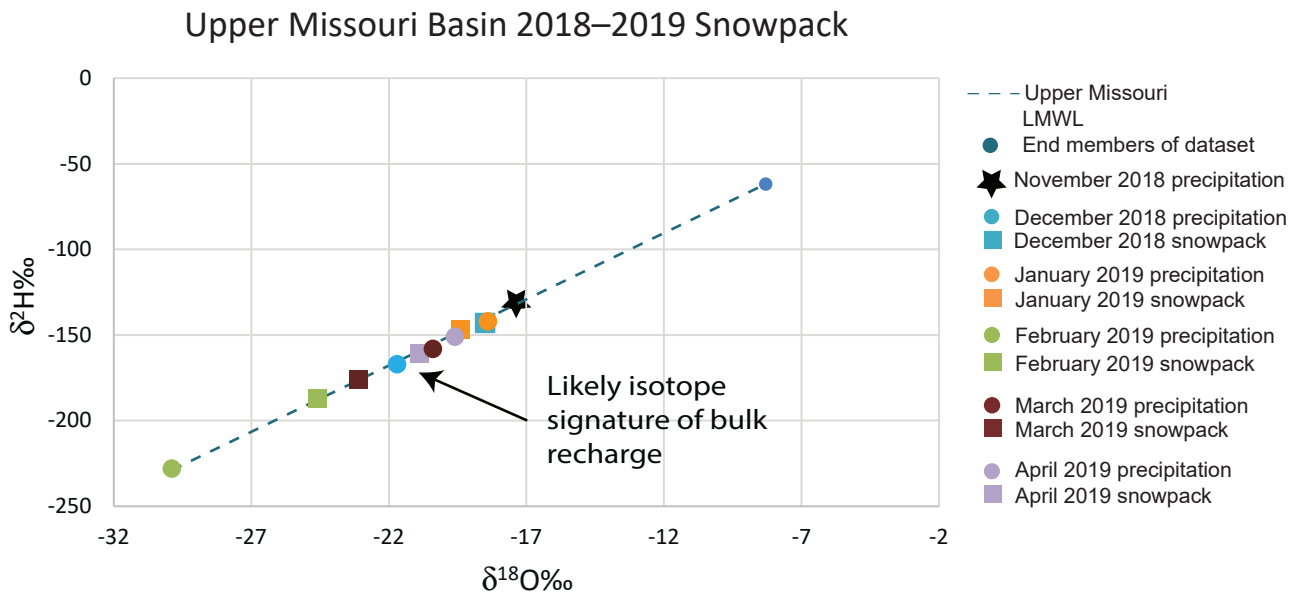

Figure 11. Winter 2018–2019 snowpack data graphed with the basin LMWL and winter precipitation values. The LMWL is marked with the dataset's lightest (winter) and heaviest (summer) end members. February's precipitaion is isotopically the lowest value.

by just 1.1‰ (within instrument error). Lolo Pass SNOTEL had a higher median *d-excess* value (8.2‰) than both Upper Lolo and Lower Lolo, which were similar (5.6‰ and 4.4‰; fig 13). Despite these differences, the LMWL regressions are similar.

The similarities of the LMWLs for each site suggest that a single LMWL for the basin is appropriate:

Bitterroot Basin–Lolo:

$$\delta^2H = 7.73\ (\pm\ 0.16)\ \delta^{18}O + 3.26\ (\pm\ 2.73).$$

The Lolo Pass SNOTEL snowpack behaves similarly to Basin Creek SNOTEL and MacDonald Pass snowpack; as it accumulates and then starts to ablate, isotopic values stay on the LMWL (fig. 14). December and January precipitation are isotopically similar, and consequently the snowpack is representative precipitation of those two months. February precipitation was isotopically lighter and shifted the snowpack signature because of February's high snowfall amount (table 3). March was a month of continued snowpack accumulation; precipitation was relatively isotopically light, but not enough in amount to shift snowpack isotopic composition. April marked the beginning of warmer temperatures and changes in snowpack mass and isotopic composition. Mid-May snowpack resembled December composition as it began a quick decline in mass, quickly moving through the ablation phase. Throughout this process the snowpack continues to plot on the LMWL.

Lolo Pass is marked by heavy, wet snowfall with an annual average of 1,170 mm (46 in), twice that of the other sites, including the high-elevation sites (Basin Creek SNOTEL and MacDonald Pass; table 1, fig. 8). Precipitation averages at Upper Lolo and Lower Lolo were 550 mm (22 in) and 487 mm (19 in), and annual values are similar to the other sites for years 2019 and 2020 (fig. 8). Of the three sites, the Upper Lolo site recorded the lowest average monthly temperature (-10°C, February 2019; fig. 9), and Lower Lolo the highest average monthly temperature (19°C, August 2020). In general, the Lolo Pass SNOTEL has a smaller interquartile temperature range than the other basin sites, but a similar median to Upper Lolo (fig. 9).

Tritium

The initial tritium results (November 2018–May 2020) from Basin Creek SNOTEL (*n = 3*), Lolo Pass SNOTEL (*n = 5*), MacDonald Pass (*n = 4*), and Lubrecht–Jones Pond (*n = 1*) varied seasonally. Spring values were between 5.2 and 15.6 TUs and fall values between 3.0 and 7.3 (appendix C). At each of these sites, the spring values were roughly double those of the fall. (Lubrecht–Jones Pond's single value was from an October composite: 3.7 TU). Monthly values (September 2020–September 2021) from Basin Creek SNOTEL and Lolo Pass SNOTEL provide better resolution of the annual variation. Basin Creek SNOTEL values varied between 4.7 TU (October 2020) and 13.3 TU (April 2021); Lolo Pass SNOTEL values var-

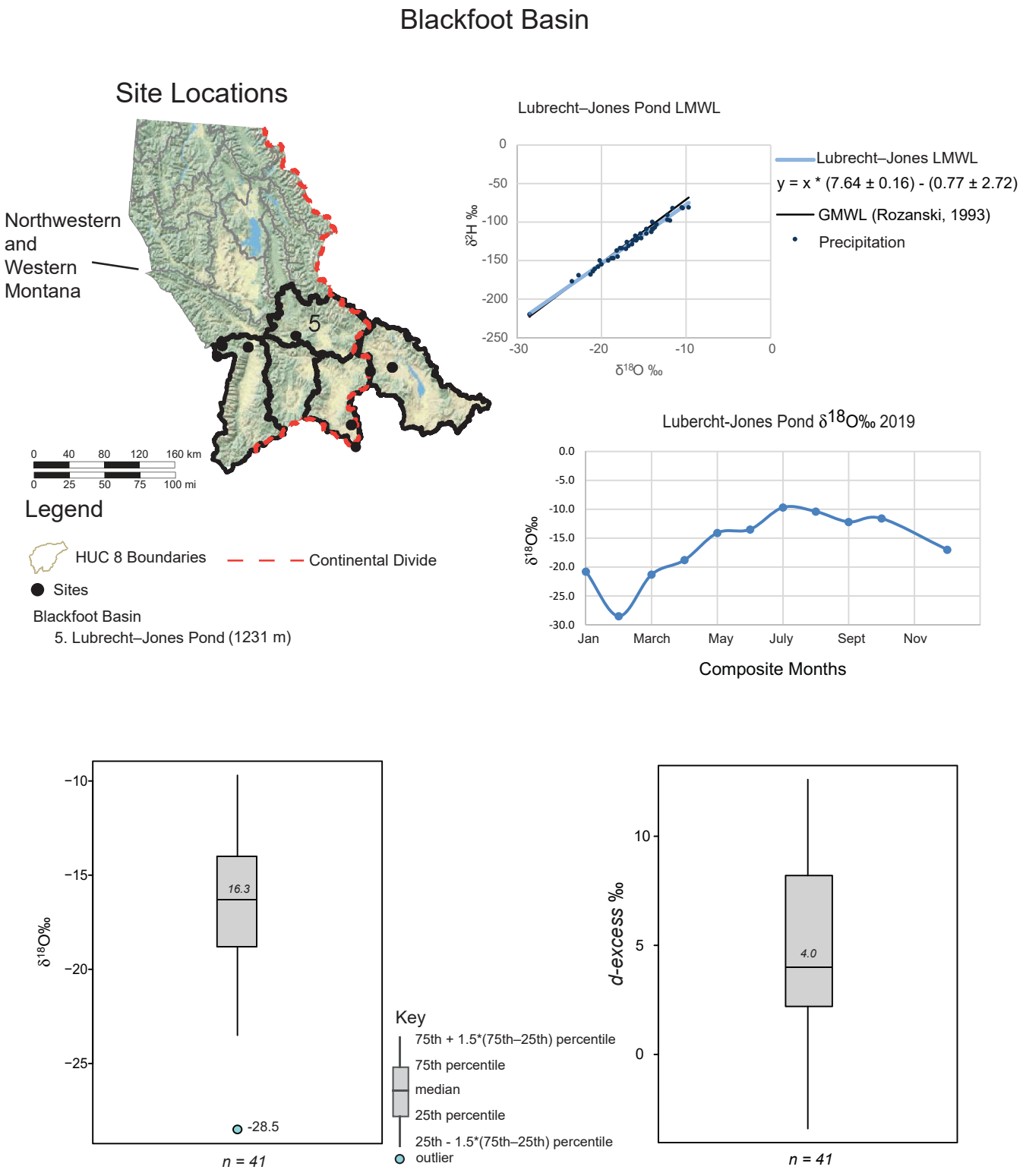

Figure 12. Lubrecht–Jones Pond is the only Blackfoot basin site. Its LMWL is graphed with the GMWL. February 2019 $\delta^{18}O$ value is labeled on the left boxplot.

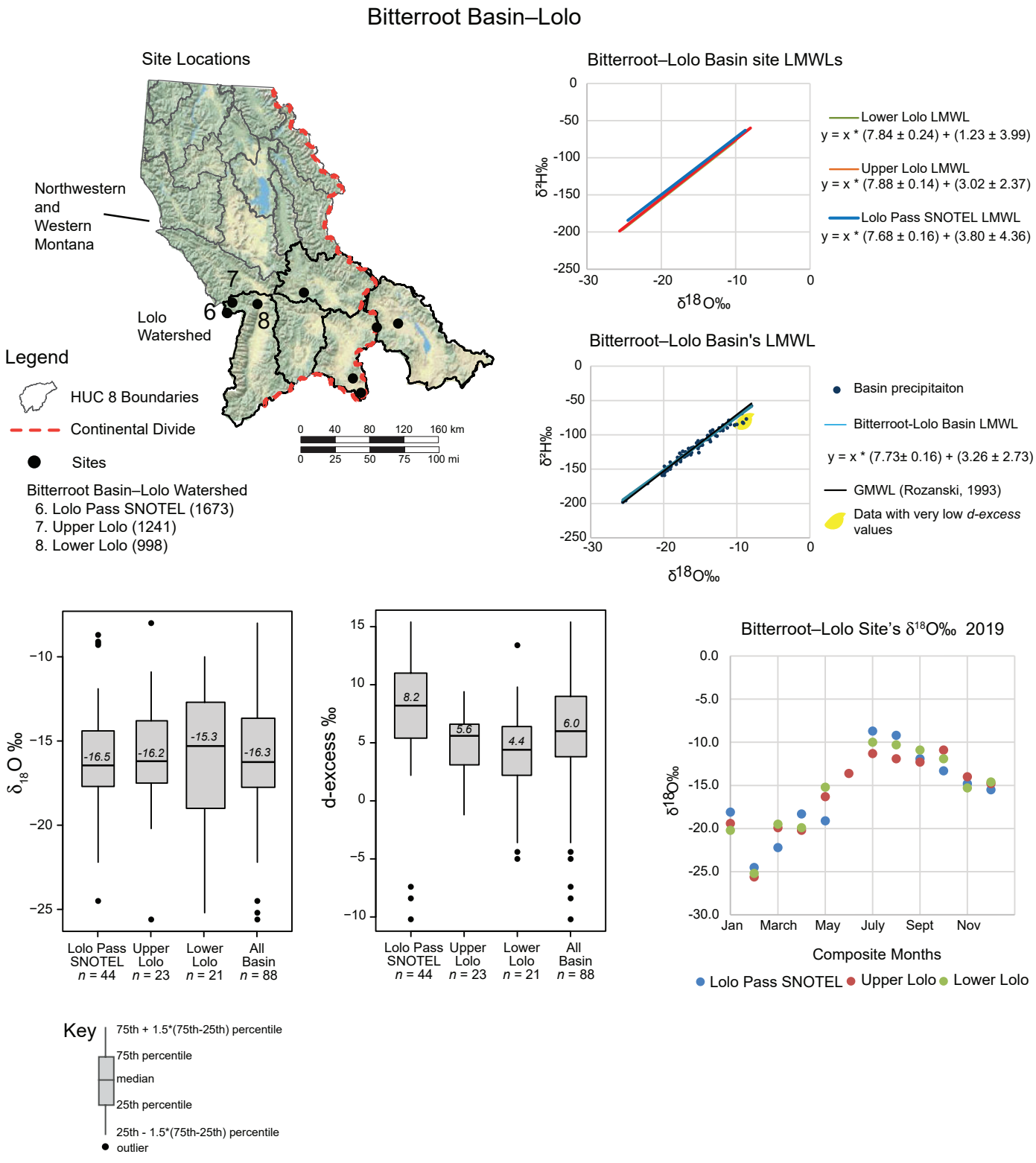

Figure 13. The Bitterroot–Lolo basin site LMWLs graphed together, and then below the combined basin LMWL graphed with GMWL and precipitation. Precipitation data from 2019 $\delta^{18}O$ values are graphed by month; to left, boxplots for entire dataset by site and grouped as a basin total.

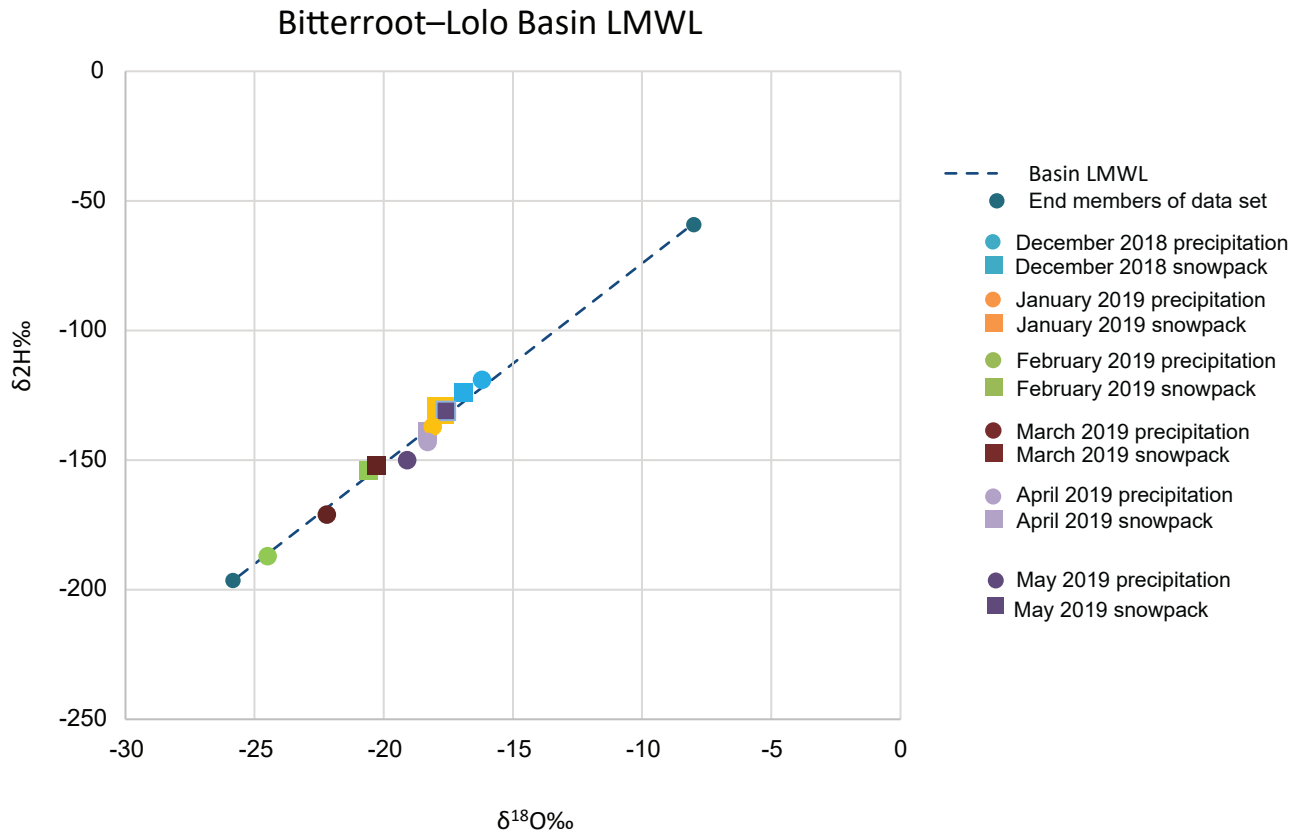

Figure 14. Winter 2018–2019 snowpack data graphed with the basin LMWL and winter precipitation values. The LMWL is marked with the dataset's lightest (winter) and heaviest (summer) end members.

ied between 3.8 TU (October 2020) and 13.8 TU (June 2021). The tritium results from all the sites ranged from 3 to 15.6 TU, with a median of 7.4 TU (fig. 15). Concentrations vary between spring–summer (March–August) and fall–winter (October–January; fig. 16).

SUMMARY AND DISCUSSION

Precipitation sampling stations were established in four basins located in western Montana to collect monthly samples for stable isotope analysis (^{2}H and ^{18}O). The area is within the northern Rocky Mountain Intermontane Basin physiographic province. The sites are located in the western climate region of Montana (Witlock and others, 2017), which is characterized by cold winters and mild summers; precipitation from moisture-rich Pacific maritime air is common in the winter, spring, and fall, and from strong convective systems in the summer. Within the basins, precipitation varies with elevation; valley bottoms typically receive less than 300 mm (12 in), whereas adjacent mountain ranges may receive more than 1,500 mm (60 in) of annual precipitation.

Western Montana Meteoric Line

The LMWLs calculated for each basin were similar. Because of this similarity, data for all the sites were combined to calculate a meteoric water line for western Montana (fig. 17; $n = 313$).

Western Montana:

$$\delta^{2}H = 7.75\ (\pm\ 0.06)\ \delta^{18}O + 2.95\ (\pm\ 1.17).$$

Basins with a high and low elevation site had elevation differences that ranged from 408 m to 775 m; between the high and low sites, there appeared to be no elevation effects or lapse rates (table 4). In general, the winter precipitation was lighter than the summer precipitation. The average $\delta^{18}O$ and $\delta^{2}H$ values from December, January, and February were -20.5‰ and -157.9‰; the June, August, and September values averaged -12.6‰; and -99.6‰ (fig. 17). The spring and fall (transition season) isotopic values overlap with winter and summer (fig. 17). All of these precipitation stations except the Helena Valley are located within one Montana climate region (western climate region; Whitlock and others, 2017).

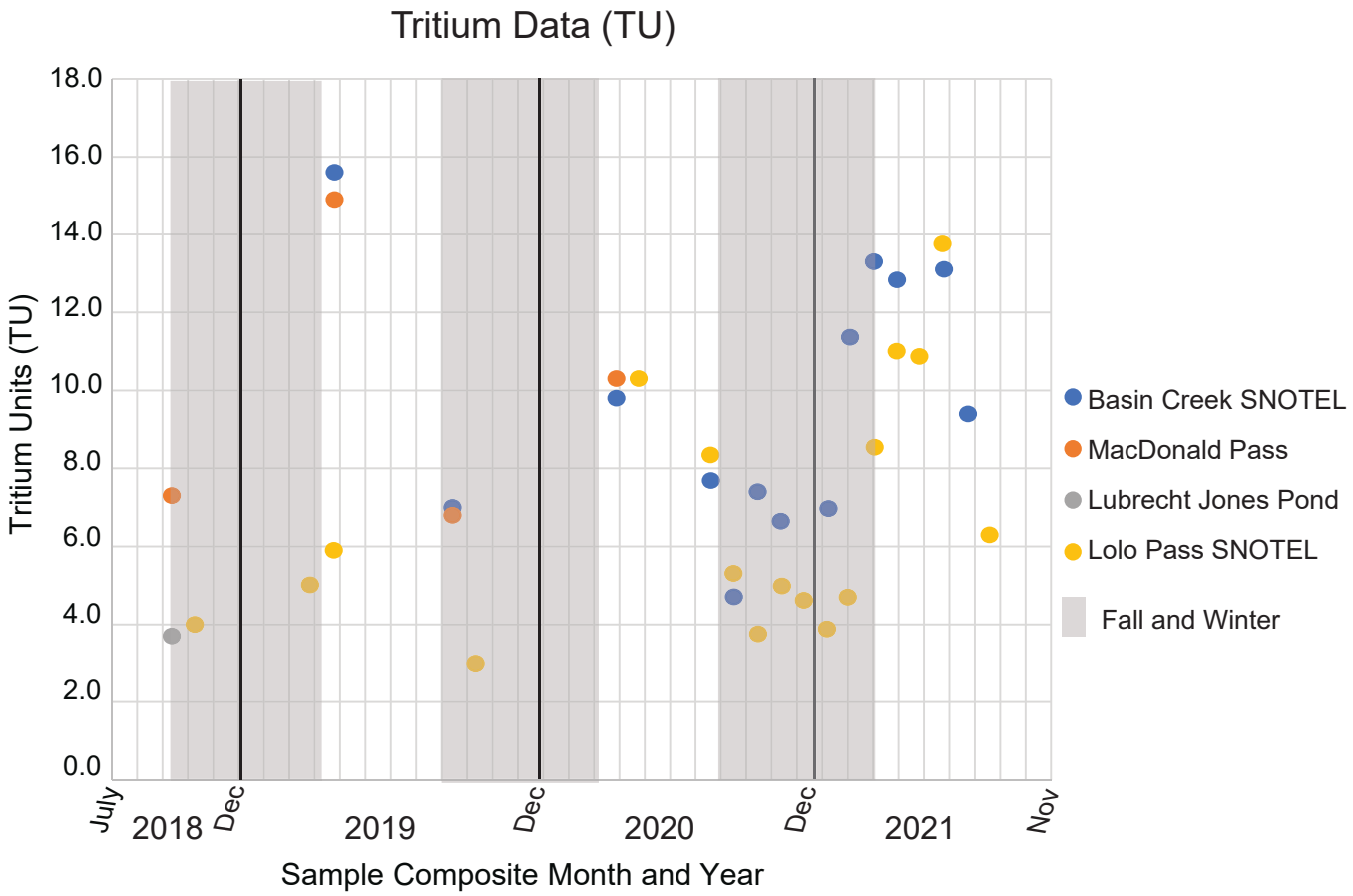

Figure 15. Tritium values from all sites are plotted by collection month and year. fall and winter are shaded gray.

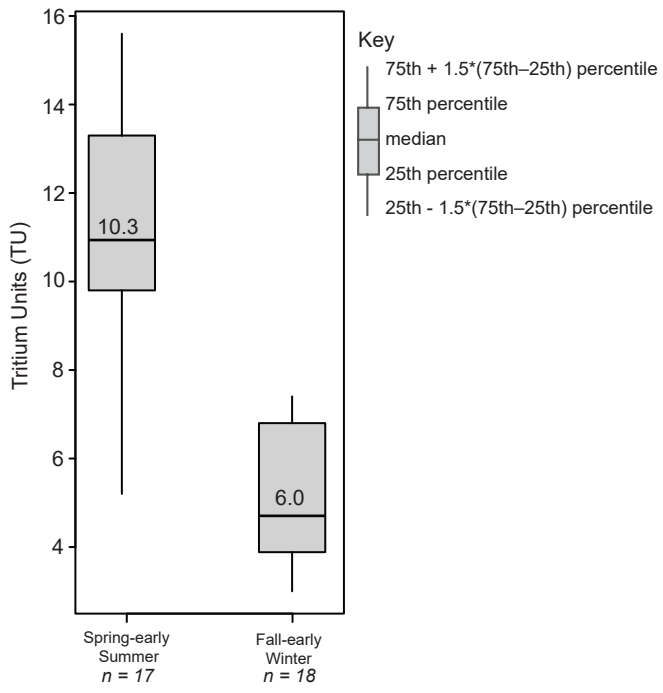

Figure 16. Tritium values plotted by season: spring–early summer (March–August) and fall–early wInter (September –January).

Comparison to Previous Work

Figure 18 compares the meteoric water line obtained in this study for western Montana with a number of previously published meteoric water lines for Montana and surrounding areas (table 5). The western Montana LMWL of this study is very similar to the global precipitation line of Rozanski and others (1993) and Benjamin and others (2004), which was based on 72 snowcore and precipitation samples collected from locations in southeastern Idaho, western Wyoming, and south-central Montana. Kharaka and others (2002) developed a LMWL for the greater Yellowstone National Park region that has a slightly steeper slope than the results of this study, whereas the local meteoric water line for Butte, Montana, obtained by Gammons and others (2006), has a less steep slope. The regression of Gammons and others (2006) was based on unweighted, precipitation-event sampling over a 12-mo period. Because the data were unweighted for precipitation amount, the derived LMWL of Gammons and others was influenced by several low-volume, mid-summer rain events with anomalously low *d-excess*

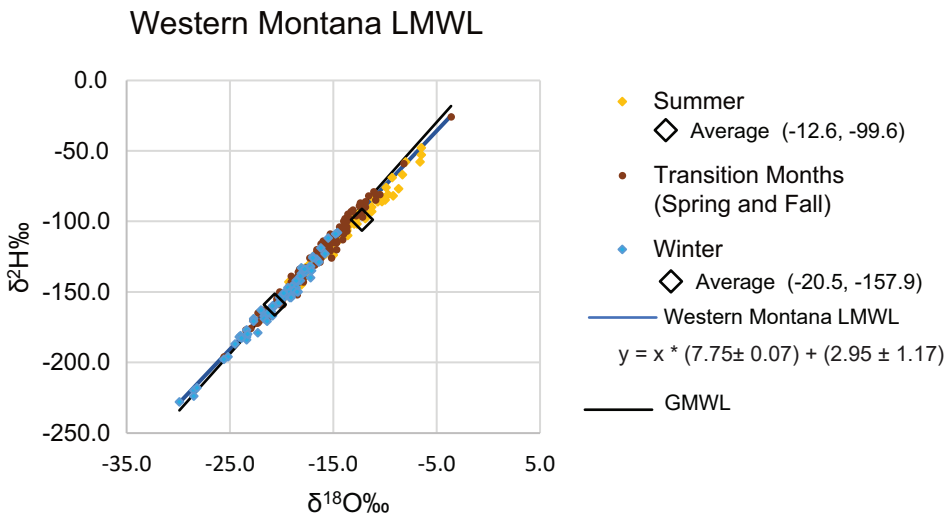

Figure 17. Graph of all precipitation data used in analysis, plotted with the Western Montana LMWL by season: summer (June, July, August), winter (December, January, February), transition (March, April, May, September, October, November).

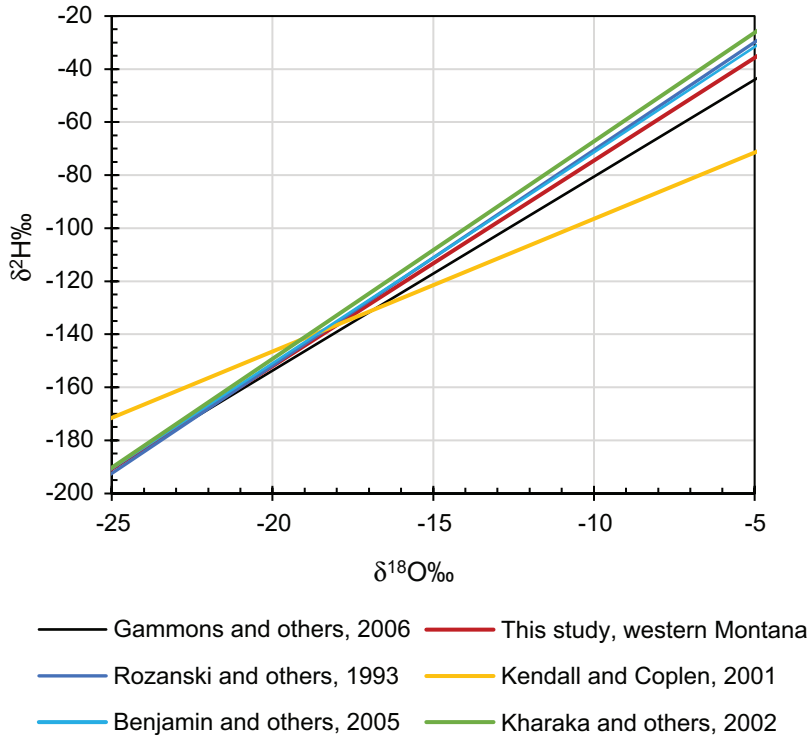

Figure 18. Graph of previous LMWLs including our Western Montana LMWL. The GMWL of Rozanski and others (1993) is also included.

Table 5. Montana Local Meteoric Water Lines.

Kendall and Coplen (2001)	$\delta^2H = 5*\delta^{18}O - 45$
Kharka and others (2002)	$\delta^2H = 8.2*\delta^{18}O + 14.7$
Benjamin and others (2004)	$\delta^2H = 7.95*\delta^{18}O + 8.09$
Gammons and others (2004)	$\delta^2H = 7.31*\delta^{18}O - 7.5$
Leuthold and others (2021)	$\delta^2H = 7.6*\delta^{18}O + 1.4$
MBMG Western Regional	$\delta^2H = 7.75 (\pm 0.06) \delta^{18}O + 2.95 (\pm 1.17)$

values. In contrast, this work used weighted monthly composite samples collected for 4 yr.

Although Kendall and Coplen (2001) published the first LMWL for Montana, their regression was based on river samples collected by the USGS National Stream Quality Accounting Network and Hydrologic Benchmark Network, many of which showed signs of significant evaporation from upstream reservoirs. Gammons and others (2006) reinterpreted the data of Kendall and Coplen (2001) as a local evaporation line (LEL), and showed that the slope of the Kendall and Coplen line was similar to the slope displayed by highly evaporated waters in the Butte area (e.g., the Berkeley Pit lake). Henderson and Shuman (2009) analyzed lake isotopes across the western United States including Montana (northwest and southwest). Their work estimates an even lower LEL line for those areas (slopes between 4.21 and 4.11; intercepts between -52.67 and -53.77).

The work completed by Leuthold and others (2021), though of short duration, differing sample protocol, and LMWL calculation, resulted in an LMWL closer in value to the western Montana regional LMWL.

Snowpack

High-elevation, composite snowpack samples collected over two winters (2018–2019 and 2019–2020) show that as the western Montana snowpack accumulates and ablates, the isotopic signature does not deviate from the LMWL. The February composite snowpack samples are generally the lightest and, in most years, mark the end of the accumulation period. The February composite values, however, are still heavier than February precipitation values, as they are also affected by the December and January precipitation signature. Snowpack samples from the ablation phase, late April or early May, when the snowpack is starting to compact and melt, are heavier, and probably represent the isotopic signature of annual recharge water. High-elevation sites can be difficult to get to and sample monthly. The results from this work suggest that a local meteoric line could be constructed with snowpack samples from February (the lightest signature) and April (to catch that recharge signature more closely) combined with the easier to collect late spring, summer, and fall precipitation samples. This methodology may not catch the lightest precipitation signature, but should yield a robust LMWL, and with the late-season snowpack sample give an indication of recharge composition. This methodology is currently being tested at the Basin Creek SNOTEL site.

Tritium

The tritium results show that concentrations in precipitation are affected by season (fig. 16); in general, there is a pronounced difference between the samples collected in the spring–summer (March–July) and the fall–winter (September–January). The median concentration of the spring–summer samples was 10.3 TU (n = 17), whereas the median concentration of the fall-winter samples was 6.0 TU (n = 18; fig. 16). Seasonal variations of tritium in precipitation reflect the annual spring breakup of the tropopause that injects relatively high ^{3}H water vapor into the troposphere, resulting in higher ^{3}H concentrations in the summer and lower ^{3}H concentrations in the winter (Terzer-Wassmuth and others, 2022; Michel and others, 2018).

Sampling Lessons Learned

Based on sampling experiences from this study, we make the following recommendations:

- A small bottle is imperative for summer precipitation collection to prevent (as much as possible) early rain events having a connection to the atmosphere after capture.
- Collector delivery tube and siphon must be switched at temperature threshold points (when temps are routinely above or below 10°C); this means replacing the tube with a siphon around October (western Montana) and swap out after March.
- Because moisture can freeze in the collector funnel neck, leading to sublimation at high-elevation western Montana sites, the GNIP HDPE 5-gal bucket performs well in December, January, and February. Otherwise, a black snow tube attachment for lower elevation sites in winter months is effective.
- The funnel neck must be cleaned out at each monthly visit.

Sample Handling

- Field bottles should be kept in a stable temperature setting and processed into lab bottles quickly.

- There should be no headspace in the 20 mL HDPE bottles.
- Duplicate samples should be collected when the precipitation amount allows; glass 20-mL bottles with a conical plastic lid can be archived for a long time.

Data Management

- Data should be analyzed in a reasonable timeframe to identify any samples that experience a random analytical error, so that a second analysis can be completed as soon as possible.

Looking Forward

This effort has collected a 4-yr robust dataset, using current global standards of collection and LMWL calculation. The results suggest that the western climate region produces, where the pilot network sites were located, a fairly common monthly average isotopic signature (fig. 17). This signature, though different, is not as different from the GMWL (fig. 17) as in some previous investigations (fig. 18).

Long-term data collection continues at three of the original pilot network sites, and additional sites in other climate regions have been established over the past several years (fig. 19). These sites have a mix of responsible parties, and include MBMG and collaborating researchers (Dr. Payton Gardner, University of Montana; Dr. Spruce Schoenemann, University of Montana Western; Dr. Stephanie Ewing, Montana State University). Some of these sites have been collecting for 3 yr, some for 6 mo. A plot of their data, plotted by climate region (fig. 20), illustrates that there might be differences across climate regional boundaries; time will tell.

Figure 20. Map of current collection MTPIN long-term network sites, 2024 (with help from collaborators) and additional precipitation sites by other researchers.

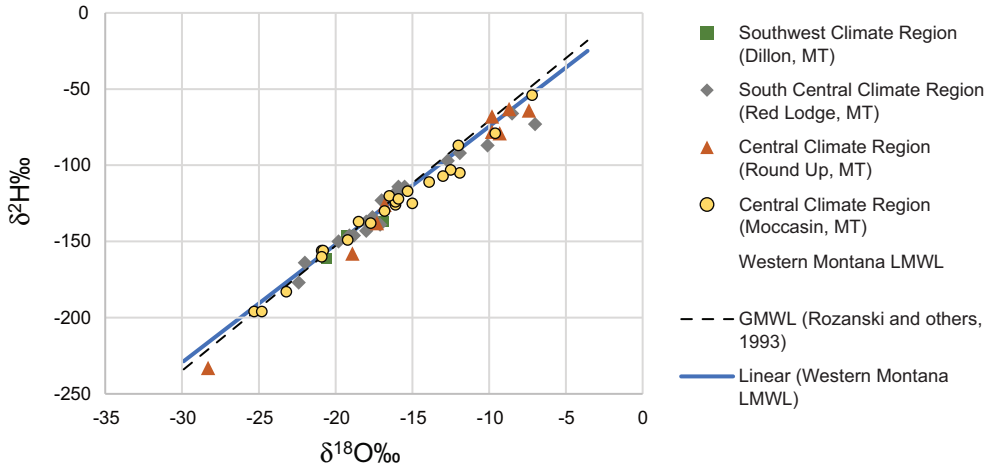

Figure 20. Montana Western Region LMWL with data from other climate regions (Southwest, South Central, Central).

ACKNOWLEDGMENTS

Through the course of the 4 years there have been numerous and important collegial relationships instrumental in the creation and maintenance of the pilot network and collection of data. These include: Dr. Payton Gardner at the University of Montana, Dr. Chris Gammons at Montana Technological University, Dr. Stephanie Ewing at Montana State University, James Swierc at Aaniih Nakoda College, and Dr. Spruce Schoenemann at University of Montana Western.

This collaboration includes other agencies (Missoula Valley Water Quality District, NWB Sensors, United States Forest Service, NRSC SNOTEL, and Montana Climate Office), Lubrecht Experimental Forest, and individuals: Kim Bolhuis, Allie Wood, Travis Ross, Jenna Rolle, David Baude, Lauren Herbine, Thomas Cope, Megan Heath, Kerrie Mueller, Amanda Rossi, Kori Riley, Craig Beebe, Josh Boyd, Austin Beard, David Callery, and Don Feist. A special thank you to landowners Cliff and Hazel Dodson and Bobbie and Barry Bartlette. Many thanks to Joanna Thamke and the Wyoming–Montana Water Science Center, Helena, Montana for providing a secure home for the Helena Valley collector.

This effort would not have gotten off the wish list without the many conversations and the support of Dr. Chris Gammons, Steve McGrath, John LaFave, Jackie Timmer, Dr. Payton Gardner, Dr. Kelsey Jencso, and Kevin Hyde. The actual collectors would not have been purchased without the help of many of the above. The work would not have been manageable without the guidance of IAEA Global Network of Isotopes in Precipitation (GNIP) and specifically Stefan Terzer-Wassmuth. Palmex, the Croatian company that manufactures the collector, was supportive and responsive to my challenges and needs (Ana Pancirov).

There are colleagues that have helped manage the data (Ann Hanson), and cheered on the effort (Dr. Dick Berg). Many thanks to the reviewers of this document, notably the efforts by Chris Gammons, Daniel Ibarra, and Ashley Huft. Susan Smith's help with figures and Susan Barth's efforts in the publication of the document are greatly appreciated.

REFERENCES

Beisner, K.R., Gardner, W.P., and Hunt, A.G., 2018, Geochemical characterization and modeling of regional groundwater contributing to the Verde River, Arizona between Mormon Pocket and the USGS Clarkdale gage: Journal of Hydrology, v. 564, p. 99–114, https://doi.org/10.1016/J.JHYDROL.2018.06.078.

Benjamin, L., Knobel, L.L., Hall, L.F.., Cecil, L.D., and Green, J.R., 2004, Development of a Local Meteoric Water Line for southeastern Idaho, western Wyoming, and south-central Montana: U.S. Geological Survey Scientific Investigations Report 2004-5126 (DOE/ID-22191), 17 p., https://doi.org/10.3133/sir20045126.

Clark, I., and Fritz, P., 1997, Environmental isotopes in hydrogeology: Boca Raton, Fla., CRC Press, 343 p., https://doi.org/10.1201/9781482242911.

Coplen, T.B., Herczeg, A.L., and Brown, C., 2000, Isotope engineering—Using stable isotopes of

water molecules to solve practical problems, *in* Cook, P.G., and Herczeg, A.L. (eds.), Environmental tracers in subsurface hydrology: Boston, Kluwer Publishers, p. 79–110, https://doi.org/10.1007/978-1-4615-4557-6_3.

Craig, H., 1961, Isotopic variations in meteoric waters: Science, v. 133, p. 1702–1703, https://doi.org/10.1126/science.133.3465.1702.

Crawford, J., Hollins, S.E., Meredith, K.T., and Hughes, C.E., 2017, Precipitation stable isotope variability and subcloud evaporation processes in a semi-arid region: Hydrological Processes, v. 31, p. 20–34, https://doi.org/10.1002/hyp.10885.

Dansgaard, W., 1964, Stable isotopes in precipitation: Tellus, v. 16, p. 436–468, https://doi.org/10.3402/tellusa.v16i4.8993.

Dansgaard, W., Johnsen, S., Clausen, H., Dahl-Jensen, D., Gunderstrup, N.S., Hammer, C.S., Hvidberg, C.S., Steffensen, J.P., Sveinbjornsdottir, A.E., Jouzel, J., and Bond, G., 1993, Evidence for general instability of past climate from a 250-kyr ice-core record: Nature, v. 364, p. 218–220, https://doi.org/10.1038/364218a0.

Evaristo, J., Jasechko, S., and McDonnell, J.J., 2015, Global separation of plant transpiration from groundwater and streamflow: Nature, v. 525, p. 91–94, https://doi.org/10.1038/nature14983.

Froehlich, K., Gibson, J.J., and Aggarwal, P., 2002, Deuterium excess in precipitation and its climatological significance: International Atomic Energy Agency, Report IAEA-CN-80/104, available at https://inis.iaea.org/search/search.aspx?orig_q=RN:34017972 [November 2024].

Gammons, C.H., Poulson, S.R., Pellicori, D.A., Reed, P.J., Roesler, A.J., and Petrescu, E.M., 2006, The hydrogen and oxygen isotopic composition of precipitation, evaporated mine water, and river water in Montana, USA: Journal of Hydrology, v. 328, p. 319–330, https://doi.org/10.1016/j.jhydrol.2005.12.005.

Gardner, W.P., Hokr, M., Shao, H., Balvin, A., Kunz, H., and Wang, Y., 2016, Investigating the age distribution of fracture discharge using multiple environmental tracers, Bedrichov Tunnel, Czech Republic: *Environmental Earth Sciences,* v. 75, p. 1374, https://doi.org/10.1007/s12665-016-6160-x.

Gröning, M., Lutz, H.O., Roller-Lutz, Z., Kralik, M., Gourcy, L., and Pöltenstein, L. 2012, A simple rain collector preventing water re-evaporation dedicated for $\delta^{18}O$ and $\delta^{2}H$ analysis of cumulative precipitation samples: Journal of Hydrology, v. 448–449, p. 195–200, https://doi.org/10.1016/j.jhydrol.2012.04.041.

Henderson, A.K., and Shuman, B.N., 2009, Hydrogen and oxygen isotopic compositions of lake water in the western United States: GSA Bulletin, v. 121, no. 7/8, p. 1179–1189, https://doi.org/10.1130/B26441.1.

Hughes, C.E., and Crawford, J., 2012, A new precipitation weighted method for determining the meteoric water line for hydrological applications demonstrated using Australian and global GNIP data: Journal of Hydrology, v. 489, p. 344–351, https://doi.org/10.1016/j.jhydrol.2012.07.029.

International Atomic Energy Agency (IAEA), 2002, A new device for monthly rainfall sampling for GNIP: Water and Environment News, v. 16, p. 5.

International Atomic Energy Agency (IAEA), 2014, IAEA/GNIP Precipitation Sampling Guide, v. 20.

Jasechko, S., 2019, Global isotope hydrogeology-review: Reviews of Geophysics, v. 57, p. 835–965, https://doi.org/10.1029/2018RG000627.

Kendall, C., and Coplen, T.B., 2001, Distribution of oxygen-18 and deuterium in river waters across the United States: Hydrological Processes, v. 15, no. 7, p. 1363–1393, https://doi.org/10.1002/hyp.217.

Kendy, E., and Tresh, R.E., 1996, Geographic, geologic, and hydrologic summaries of intermontane basins of the northern Rocky Mountains, Montana: U.S. Geological Survey Water Resources Investigations Report 96-4025, 233 p., https://doi.org/10.3133/wri964025.

Kharaka, Y.K., Thordson, J.J., and White, L.D., 2002, Isotope and chemical compositions of meteoric and thermal waters and snow from the great Yellowstone National Park region: U.S. Geological Survey Open-File Report 02-194, 18 p.

Kreutz, K.J., Wake, C.P., Aizen, V.B., Cecil, L.D., and Synal, H.A., 2003, Seasonal deuterium excess in a Tien Shan ice core: Influence of moisture transport and recycling in Central Asia: Geophysical

Research Letters, v. 30, no. 18, p. 1922, https://doi.org/10.1029/2003 GL 17896.

Leuthold, S.J., Ewing, S.A., Payn, R.A., Miller, F.R., and Custer, S.G., 2021, Seasonal connections between meteoric water and streamflow generation along a mountain headwater stream: Hydrological Processes, v. 35, no. 2, p. 1–17, https://doi.org/10.1002/hyp.14029.

Lindsey, B.D., Jurgens, B.C., and Belitz, K., 2019, Tritium as an indicator of modern, mixed, and premodern groundwater age: U.S. Geological Survey Scientific Investigations Report 2019–5090, 18 p., https://doi.org/10.3133/sir20195090.

McDonnell, J. J., Stewart, M. K., & Owens, I. F. (1991). Effect of Catchment-Scale Subsurface Mixing on Stream Isotopic Response. *Water Resources Research*, *27*(12), 3065–3073. https://doi.org/10.1029/91WR02025

McDonnell, J.J., and Klaus, J., 2015, Hydrograph separation using stable isotopes: Review and evaluation: Journal of Hydrology, v. 505, p. 47–64, https://doi.org/10.1016/j.jhydrol.2013.09.006.

McGuire, K., and McDonnell, J., 2007, Stable isotope tracers in watershed hydrology, *in* Stable isotopes in ecology and environmental science, Michener, R., and Lajita, K., eds.: Malden, MA, Blackwell Publishing, Ch. 11, p. 334–373, https://doi.org/10.1002/9780470691854.ch11.

Michel, R.L., Jurgens, B.C., and Young, M.B., 2018, Tritium deposition in precipitation in the United States, 1953–2012: U.S. Geological Survey Scientific Investigations Report 2018–5086, 11 p., https://doi.org/10.3133/sir20185086.

Michelsen, N., van Geldern, R., Roßmann, Y., Bauer, I., Schulz, S., Barth, J.A., and Schüth, C., 2018, Comparison of precipitation collectors used in isotope hydrology: Chemical Geology, v. 488, p. 171–179, https://doi.org/10.1016/j.chemgeo.2018.04.032.

Putnam, A.L., Fiorella, R.P., Bowen, G.J., and Cai, Z., 2019, A global perspective on local meteoric water lines: Meta-analytic insight into fundamental controls and practical constraints: Water Resources Research, v. 55, p. 6896–6910, https://doi.org/10.1029/2019WR025181.

Rozanski, K., Araguás-Araguás, L., and Gonfiantini, R., 1993, Isotopic patterns in modern global precipitation, *in* Swart, P.K., Lohmann, K.C., McKenzie, J., and Savin, S., eds., Climate change in continental isotopic records, Geophysical Monograph 78: Washington, D.C., American Geophysical Union, p. 1–36, https://doi.org/10.1029/GM078p0001.

Rye, R.O., and Truesdell, A.H., 1993, The question of recharge to the geysers and hot springs of Yellowstone National Park: U.S. Geological Survey Open-File Report, v. 93-384, https://doi.org/10.3133/ofr93384.

Sklash, M.G., and Farvolden, R.N., 1979, The role of groundwater in storm runoff: Journal of Hydrology, v. 43, p. 45–65, https://doi.org/10.1016/0022-1694(79)90164-1.

Solomon, D.K., and Cook, P.G., 2000, ^{3}H And ^{3}He, *in* Cook, P.G., and Herczeg, A.L., eds., Environmental tracers in subsurface hydrology: Boston, Kluwer Publishers, p. 397–439.

Terzer-Wassmuth, S., Araguás-Araguás, L.J., Copia, L., and Wassenaar, L.I., 2022, High spatial resolution prediction of tritium (^{3}H) in contemporary global precipitation: Scientific Reports, v. 12, no. 1, p. 10271, https://doi.org/10.1038/s41598-022-14227-5.

Wang, S., Zhang, M., Hughes, C.E., Crawford, J., Wang, G., Chen, F., Du, M., Qiu, X., and Zhou, S., 2018, Meteoric water lines in arid Central Asia using event-based and monthly data: Journal of Hydrology, v. 562, p. 435–445, https://doi.org/10.1016/j.jhydrol.2018.05.034.

Whitlock, C., Cross, W., Maxwell, B., Silverman, N., and Wade, A.A., 2017, 2017 Montana Climate Assessment: Bozeman and Missoula, Mont., Montana State University and University of Montana, Montana Institute on Ecosystems, 318 p., https://doi.org/10.15788/m2ww8w.

APPENDIX A: SITE DATA

Appendix A. Dataset used for report analysis.

Sample Date	Method	Precipitation (mm)	Temp average °C	Vapor Pressure (kPa)	Sample ID	$d^{18}O$ ‰	$d^{2}H$ ‰	*d-excess*
UPPER CLARK FORK BASIN								
MBMG: GNIP station 727401, GWIC ID 297504, 46.01378, 112.561, 1,762 m								
12/2/18	Collector	23	-1.66	0.25	236438	-22.3	-171.0	7.4
1/3/19	Collector	19	-5.32	0.15	237480	-20.9	-167.0	0.2
1/30/19	Collector	9	-4.06	0.16	238582	-19.2	-154.0	-0.4
2/28/19	Collector	37	-11.54	0.07	238660	-28.5	-224.0	4.0
3/30/19	Collector	30	-4.86	0.15	238713	-18.7	-143.0	6.6
5/1/19	Collector	45	3.45	0.30	238777	-17.9	-137.0	6.2
6/1/29	Collector	47	7.39	0.45	238883	-17.8	-135.0	7.4
6/30/19	Collector	20	12.53	0.73	238984	-13.0	-102.0	2.0
7/30/19	Collector	27	17.09	1.13	239114	-10.5	-82.0	2.0
8/29/19	Collector	28	17.83	1.27	240373	-10.7	-83.0	2.6
9/30/19	Collector	68	11.66	0.79	243455	-12.4	-87.0	12.2
11/2/19	Collector	20	-0.28	0.30	243508	-17.6	-133.0	7.8
11/30/19	Collector	19	-1.15	0.25	243596	-25.6	-196.0	8.8
1/2/20	Collector	8	-3.57	0.16	243647	-20.3	-158.0	4.4
2/1/20	Collector	4.1	-2.92	0.17	243793	-18.5	-150.0	-2.0
2/27/20	Collector	15	-4.26	0.17	243835	-19.1	-154.0	-1.2
4/1/20	Collector	20	-1.26	0.23	243920	-18.2	-137.0	8.6
4/1/20	Collector	20	-1.26	0.23	243921	-17.8	-134.0	8.4
4/28/20	Collector	20	2.94	0.44	244967	-21.1	-162.0	6.8
6/1/20	Collector	46	8.50	0.55	246033	-13.7	-104.0	5.6
6/29/20	Collector	89	12.11	0.72	246387	-17.4	-131.0	8.2
8/2/20	Collector	18	16.96	1.14	248465	-12.6	-97.0	3.8
9/2/20	Collector	7	18.62	1.43	249594	-2.2	-53.0	-35.4
9/28/20	Collector	19	13.80	1.12	251697	-15.9	-119.0	8.2
11/1/20	Collector	25	4.73	0.53	251778	-16.0	-114.0	14.0
11/28/20	Collector	16	-0.49	0.30	251901	-21.0	-161.0	7.0
12/30/20	Collector	68	-3.07	0.18	251906	-23.4	-184.0	3.2
1/28/21	Collector	53	-3.50	0.16	252125	-17.2	-140.0	-2.4
2/25/21	Collector	36	-8.44	0.09	252140	-21.4	-171.0	0.2
3/31/21	Collector	9	-0.04	0.27	252193	-17.9	-140.0	3.2
5/1/21	Collector	11	2.99	0.44	252294	-15.9	-120.0	7.2
6/1/21	Collector	30	7.22	0.56	252537	-15.9	-117.0	10.2
7/3/21	Collector	23	17.43	1.33	252555	-15.7	-123.0	2.6
8/2/21	Collector	31	21.52	1.77	252840	-6.5	-48.0	4.0
9/1/21	Collector	46	16.34	1.04	252843	-14.6	-110.0	6.8
9/30/21	Collector	3	13.58	1.08	253113	-3.6	-26.0	2.8
10/29/21	Collector	7	6.32	0.49	253119	-18.6	-169.0	-20.2
11/30/21	Collector	20	1.87	0.31	253252	-13.9	-101.0	10.2
1/3/22	Collector	15	-3.60	0.17	253261	-23.3	-180	6.4
1/30/22	Collector	18	-4.18	0.16	253265	-23.9	-183	8.2
2/28/22	Collector	7	-5.22	0.18	253577	-22.3	-179	-0.6
4/1/22	Collector	8	0.51	0.30	253579	-15.3	-116	6.4
5/1/22	Collector	28	-0.29	0.28	253581	-18.6	-140	8.8

Sample Date	Method	Precipitation (mm)	Temp average °C	Vapor Pressure (kPa)	Sample ID	$d^{18}O$ ‰	$d^{2}H$ ‰	*d-excess*
5/30/22	Collector	68	6.35	0.41	253583	-21.7	-168	5.6
7/2/22	Collector	54	12.65	0.71	253663	-14.8	-114	4.4
8/1/22	Collector	36	19.49	1.38	254013	-10.2	-85	-3.4
8/30/22	Collector	30	20.22	1.56	254018	-6.6	-58	-5.2
10/1/22	Collector	45	14.81	1.04	254022	-12.8	-96	6.4
10/31/22	Collector	4.8	7.56	0.49	255168	-22.4	-172	7.2
11/28/22	Collector	12	-6.29	0.12	255217	-22.5	-172	8.0
Basin Creek SNOTEL GNIP Station 7277402, GWIC ID 298870-Collector, 304005-Bucket, 45.79718, 112.521, 2,170 m								
12/2/18	Collector	35	-1.72		236441	-19.3	-146	8.4
1/2/19	Collector	27	-5.56		237494	-18.3	-149	-2.6
1/2/19	Bucket	26	-5.56		237495	-19.1	-153	-0.2
1/30/19	Collector	30	-3.11		238583	-19.4	-151	4.2
1/30/19	Bucket	31	-3.11		238584	-19.8	-151	7.4
2/27/19	Collector	63	-9.50		238657	-27.9	-216	7.2
2/27/19	Bucket	82	-9.50		238658	-28.2	-218	7.6
3/31/19	Collector	54	-3.56		238710	-21.1	-162	6.8
3/31/19	Bucket	18.5	-3.56		238712	-19.9	-154	5.2
5/1/19	Collector	73	2.17		238775	-18	-137	7.0
6/1/19	Collector	104	5.56		238882	-18.1	-137	7.8
6/30/19	Collector	41	10.00		238983	-13.7	-106	3.6
7/30/19	Collector	43	14.22		239113	-13.4	-101	6.2
8/29/19	Collector	33	14.17		240372	-11.1	-84	4.8
9/2/19	Collector	61	9.00		243458	-13.6	-97	11.8
11/2/19	Collector	52	-1.28		243507	-19.1	-139	13.8
11/29/19	Collector	22	-1.67		243597	-20	-150	10.0
11/29/19	Bucket	20	-1.67		243598	-20.4	-153	10.2
1/2/20	Collector	24	-3.83		243644	-20.9	-163	4.2
1/2/20	Bucket	29	-3.83		243645	-23.4	-182	5.2
2/1/20	Collector	16	-3.61		243794	-17.4	-144	-4.8
2/1/20	Bucket	15	-3.61		243795	-18.4	-150	-2.8
2/27/20	Collector	50	-5.11		243834	-18.6	-142	6.8
2/28/20	Bucket	55	-5.11		243838	-18.2	-139	6.6
4/2/20	Collector	48	-2.11		243922	-18.3	-138	8.4
4/2/20	Bucket	46	-2.11		243923	-18	-139	5.0
4/28/20	Collector	30	1.33		244965	-23.7	-182	7.6
6/1/20	Collector	50	6.72		246032	-15.2	-115	6.6
6/29/20	Collector	125	9.94		246388	-19.3	-143	11.4
8/2/20	Collector	24	14.56		248464	-12.6	-95	5.8
9/2/20	Collector	10	15.56		249593	-12.9	-97	6.2
9/28/20	Collector	33	11.00		251696	-18.4	-136	11.2
11/1/20	Collector	22	3.33		251777	-17.3	-126	12.4
11/28/20	Collector	24	-1.56		251902	-19.1	-143	9.8
12/30/20	Bucket	17	-3.28		251907	-21.3	-165	5.4
1/28/21	Bucket	12	-4.11		252126	-13.5	-116	-8.0

Sample Date	Method	Precipitation (mm)	Temp average °C	Vapor Pressure (kPa)	Sample ID	$d^{18}O$ ‰	$d^{2}H$ ‰	*d-excess*
2/25/21	Bucket	75	-8.06		252138	-23.3	-180	6.4
3/31/21	Collector	18	-1.11		252194	-17.9	-143	0.2
3/31/21	Bucket	18.6	-1.11		252195	-13.7	-120	-10.4
5/1/21	Collector	37	1.50		252296	-20.5	-155	9.0
6/1/21	Collector	36	5.56		252538	-15.2	-112	9.6
7/3/21	Collector	13	15.28		252556	-14.8	-110	8.4
8/2/21	Collector	20	18.33		252839	-9.9	-76	3.2
9/1/21	Collector	42	13.67		252844	-15.7	-115	10.6
9/30/21	Collector	8	10.94		253112	-8.2	-59	6.6
10/29/21	Collector	59	3.89		253120	-17.9	-136	7.2
11/30/21	Collector	22	0.83		253253	-14.6	-109	7.8
11/30/21	Bucket	8	0.83			No sample: Bucket melted and froze		
1/3/22	Bucket	15	-4.67		253262	-24	-181	11.0
1/30/22	Bucket	26	-3.39		253264	-23.5	-182	6.0
2/28/22	Bucket	25	-5.50		253431	-22.7	-171	10.6
4/1/22	Collector	45	-1.06		253578	-17.7	-135	6.6
4/1/22	Bucket	39	-1.06			No sample: Bucket melted and froze		
5/1/22	Collector	82	-1.28		253580	-18.4	-139	8.2
5/30/22	Collector	105	4.39		253582	-20.4	-155	8.2
7/2/22	Collector	66	10.39		253662	-16.9	-128	7.2
8/1/22	Collector	26	16.72		254012	-11.3	-93	-2.6
8/30/22	Collector	33	16.94		254017	-6.5	-53	-1.0
10/1/22	Collector	60	12.06		254021	-13.7	-100	9.6
10/31/22	Collector	30	5.39		255167	-23	-176	8.0
11/28/22	Collector	32	-5.61		255216	-21.8	-163	11.4
UPPER MISSOURI BASIN								
Helena Valley: GNIP station 7277200, GWIC ID 298826, 46.61218, 111.988, 1,160 m								
12/3/18	Collector	2.8	-0.50	0.46	236444	-22.1	-174.0	2.8
1/10/19	Collector	1.4	-2.89	0.36	238496	-20.1	-166.0	-5.2
1/31/19	Collector	10	-4.44	0.35	238586	-18.3	-145.0	1.4
2/28/19	Collector	24	-12.94	0.17	238661	-28.3	-223.0	3.4
4/1/19	Collector	20	-5.11	0.29	238714	-20.2	-156.0	5.6
5/2/19	Collector	27	7.39	0.61	238778	-17.0	-135.0	1.0
5/31/19	Collector	43	10.89	0.68	238880	-16.4	-124.0	7.2
7/1/19	Collector	12	16.33	0.93	238985	-10.7	-90.0	-4.4
8/2/19	Collector	41	18.94	1.20	239125	-11.2	-91.0	-1.4
8/29/19	Collector	28	19.00	1.45	240374	-12.2	-91.0	6.6
10/1/19	Collector	78	12.78	0.93	243456	-13.6	-99.0	9.8
11/1/19	Collector	19	2.33	0.45	243506	-17.8	-133.0	9.4
11/27/19	Collector	5	-0.33	0.37	243600	-20.1	-149.0	11.8
1/3/20	Collector	7	-2.00	0.37	243648	-23.9	-185.0	6.2

Sample Date	Method	Precipitation (mm)	Temp average °C	Vapor Pressure (kPa)	Sample ID	$d^{18}O$ ‰	$d^{2}H$ ‰	*d-excess*
1/30/20	Collector	1.8	-1.50	0.37	243784	-20.2	-160.0	1.6
2/28/20	Collector	4	-0.39	0.36	243836	-18.0	-139.0	5.0
4/3/20	Collector	17	1.28	0.38	243925	-19.2	-148.0	5.6
5/1/20	Collector	15	6.22	0.49	244968	-16.8	-132.0	2.4
6/2/20	Collector	39	12.50	0.77	246034	-12.5	-91.0	9.0
7/2/20	Collector	85	16.17	1.05	246407	-16.1	-123.0	5.8
8/3/20	Collector	10	19.50	1.06	248466	-10.9	-94.0	-6.8
9/2/20	Collector	1	21.56	1.08	249600	2.0	-46.0	-62.0
10/2/20	Collector	11	16.05	0.93	251704	-12.8	-126.0	-23.6
11/2/20	Collector	41	1.50	0.46	251780	-19.0	-136.0	16.0
12/1/20	Collector	18	2.33	0.46	251908	-22.3	-171.0	7.4
1/4/21	Collector	11	-1.33	0.38	251911	-19.8	-152.0	6.4
2/1/21	Collector	10	-1.83	0.35	252133	-18.8	-144.0	6.4
3/2/21	Collector	20	-6.83	0.24	252145	-20.0	-160.0	0.0
4/1/21	Collector	12	2.66	0.45	252299	-17.3	-133.0	5.4
5/3/21	Collector	35	5.17	0.49	252300	-19.0	-144.0	8.0
5/28/21	Collector	62	11.78	0.68	252534	-15.1	-113.0	7.8
6/30/21	Collector	16	20.33	1.00	252552	-14.3	-107.0	7.4
8/2/21	Collector	9	25.11	1.15	253111	-4.7	-49.0	-11.4
9/2/21	Collector	47	18.56	1.34	253118	-14.4	-110.0	5.2
9/30/21	Collector	0	14.56	0.89	n/a	n/a	n/a	
11/1/21	Collector	12	8.11	0.69	253370	-16.2	-129.0	0.6
12/2/21	Collector	9	2.89	0.49	253372	-15.3	-118.0	4.4
1/4/22	Collector	16	-4.50	0.31	253375	-18.4	-141.0	6.2
2/4/22	Collector	17	-3.39	0.30	253597	-24.8	-195	3.4
3/1/22	Collector	3	-3.61	0.29	253599	-15.2	-120	1.6
4/6/22	Collector	11	2.72	0.44	253601	-15.3	-124	-1.6
5/3/22	Collector	21	2.06	0.42	253603	-15.7	-123	2.6
5/31/22	Collector	29	9.56	0.67	255174	-18.6	-149	-0.2
6/28/22	Collector	37	15.39	0.98	255176	-14.6	-117	-0.2
8/4/22	Collector	40	21.67	1.24	255178	-13.2	-102	3.6
9/6/22	Collector	16	22.94	1.12	255180	-9	-73	-1.0
10/1/22	Collector	65	16.56	0.98	255163	-11.1	-81	7.8
11/3/22	Collector	37	9.06	0.75	255215	-20.8	-161	5.4
11/29/22	Collector	21	-6.22	0.28	255222	-22.2	-171	6.6
MacDonald Pass: GNIP station 7277201, GWIC ID 298420-Collector 304011-Bucket, 46.56434, 112.308, 1,935 m								
12/3/18	Collector	55	-3.10	0.35	236439	-17.7	-133	8.6
12/3/18	Bucket	54	-3.10	0.35	236440	-17.5	-134	6.0
1/1/19	Collector	26	-6.09	0.30	237491	-18.5	-149	-1.0
1/1/19	Bucket	42	-6.09	0.30	237492	-21.7	-167	6.6
1/31/19	Collector	52	-4.74	0.33	238587	-18.7	-143	6.6
1/31/19	Bucket	52	-4.74	0.33	238588	-18.4	-142	5.2
2/28/19	Collector	95	-15.85	0.26	238662	-28.5	-221	7.0
2/28/19	Bucket	140	-15.85	0.26	238663	-29.9	-228	11.2

Sample Date	Method	Precipitation (mm)	Temp average °C	Vapor Pressure (kPa)	Sample ID	$d^{18}O$ ‰	$d^{2}H$ ‰	*d-excess*
4/1/19	Collector	50	-5.96	0.28	238715	-20.4	-158	5.2
4/1/19	Bucket	Not measured	-5.96		238716	-19	-149	3.0
5/2/19	Collector	80	0.55	0.34	238779	-19.6	-151	5.8
5/31/19	Collector	76	4.64	0.40	238881	-18.2	-139	6.6
7/1/19	Collector	15	10.53	0.47	238986	-10.7	-86	-0.4
8/2/19	Collector	45	14.36	0.55	239126	-10.7	-86	-0.4
8/29/19	Collector	33	15.21	0.59	240375	-10.9	-82	5.2
10/1/19	Collector	85	9.06	0.61	243457	-14.4	-104	11.2
11/1/19	Collector	71	-2.37	0.57	243504	-18.3	-134	12.4
11/27/19	Collector	24	-3.79	0.55	243593	-16.6	-122	10.8
11/27/19	Bucket	17	-3.79	0.55	243594	-14.8	-109	9.4
1/3/20	Collector	42	-4.07	0.52	243649	-23.4	-177	10.2
1/3/20	Bucket	37	-4.07	0.52	243650	-21.2	-162	7.6
1/30/20	Collector	22	-4.40	0.10	243785	-18.2	-142	3.6
1/30/20	Bucket	22	-4.40	0.10	243786	-17.3	-136	2.4
1/30/20	Bucket	25	-4.40	0.10	243797	-18	-140	4.0
1/30/20	Bucket	22	-4.40	0.10	243798	-18	-140	4.0
2/28/20	Collector	35	-5.75	0.11	243837	-17.1	-131	5.8
2/28/20	Bucket	75	-5.75	0.11	243851	-18.2	-139	6.6
4/3/20	Collector	64	-4.42	0.15	243926	-18.1	-141	3.8
4/3/20	Bucket	85	-4.42	0.15	243927	-19.2	-146	7.6
5/1/20	Collector	50	-0.23	0.27	244969	-19.1	-146	6.8
6/2/20	Collector	63	5.51	0.30	246035	-14	-105	7.0
7/2/20	Collector	106	9.56	0.45	246408	-16.8	-124	10.4
8/3/20	Collector	4	14.67	0.82	248467	-9.5	-85	-9.0
9/2/20	Collector	9	16.78	1.14	249599	-8.3	-67	-0.6
10/1/20	Collector	28	11.85	0.84	251705	-13.8	-152	-41.6
11/2/20	Collector	93	1.94	0.36	251779	-16.2	-116	13.6
12/1/20	Collector	42	-2.05	0.22	251909	-22.3	-165	13.4
12/1/20	Bucket	52	-2.05	0.22	251910	-20.9	-155	12.2
1/4/21	Bucket	26	-3.49	0.15	251912	-18.8	-149	1.4
2/1/21	Bucket	41	-2.60	0.13	252132	-15.8	-123	3.4
3/2/21	Bucket	94	N/A	0.31	252143	-20.9	-160	7.2
4/1/21	Collector	28	-1.30	0.21	252297	-14.7	-120	-2.4
5/1/21	Collector	38	0.20	0.27	252298	-18.5	-152	-4.0
5/28/21	Collector	58	4.55	0.35	252535	-15.2	-114	7.6
6/30/21	Collector	23	14.34	0.85	252553	-14.1	-111	1.8
8/2/21	Collector	11	19.71	1.40	253110	-5.7	-50	-4.4
9/2/21	Collector	49	14.20	0.80	253117	-15.9	-119	8.2
9/30/21	Collector	18	11.69	0.83	253136	-12.5	-89	11.0
11/1/21	Collector	33	4.53	0.54	253371	-18.9	-142	9.2
12/2/21	Collector	36	-0.27	0.46	253373	-13.9	-98	13.2
12/2/21	Bucket	40	-0.27	0.46	253374	-9.9	-73	6.2
1/4/22	Bucket	102	-7.20	0.30	253376	-22	-163	13.0
2/4/22	Bucket	57	-5.44	0.28	253596	-21.7	-169	4.6

Sample Date	Method	Precipitation (mm)	Temp average °C	Vapor Pressure (kPa)	Sample ID	$d^{18}O$ ‰	$d^{2}H$ ‰	*d-excess*
3/1/22	Bucket	51	-7.27	0.27	253598	-24.1	-182	10.8
3/30/22	Bucket	73	-2.25	0.41	253600	-19.4	-151	4.2
5/3/22	Collector	41	-2.87	0.62	253602	-17.6	-135	5.8
5/31/22	Collector	55	3.77	0.59	255173	-19.4	-148	7.2
6/28/22	Collector	68	9.90	0.61	255175	-15	-124	-4.0
8/4/22	Collector	94	16.82	1.07	255177	-15.3	-112	10.4
9/4/22	Collector	13	18.14	0.93	255179	-7.9	-72	-8.8
10/1/22	Collector	74	12.96	0.74	255164	-13.1	-92	12.8
11/3/22	Collector	24	5.92	0.49	255214	-22.3	-172	6.4
12/5/22	Collector	50	-7.76	0.26	255218	-22.8	-170	12.4
BLACKFOOT BASIN								
Lubrecht–Jones Pond: GNIP station 7277301, GWIC ID 297503-Collector 304014-Bucket, 46.8945, 113.44, 1,231 m								
11/30/18	Collector	73	-2.05	0.13	236442	-17.6	-134	6.8
12/30/18	Collector	23	-5.48	0.12	237482	-19.2	-150	3.6
2/1/19	Collector	39	-5.18	0.26	238590	-20.8	-161	5.4
3/1/19	Collector	72	-11.70	0.05	238665	-27.1	-212	4.8
3/1/19	Bucket	84	-11.70	0.05	238666	-28.5	-220	8.0
3/29/19	Collector	9	-4.32	0.18	238722	-21.3	-168	2.4
3/29/19	Bucket	10	-4.32	0.18	238723	-19.9	-158	1.2
4/29/19	Collector	73	4.09	0.29	238770	-18.8	-147	3.4
5/29/19	Collector	57	8.67	0.49	238869	-14.1	-113	-0.2
7/2/19	Collector	48	13.29	0.75	238990	-13.5	-103	5.0
8/3/19	Collector	37	16.12	1.02	239127	-9.7	-81	-3.4
8/29/19	Collector	18	16.69	1.17	240376	-10.4	-82	1.2
10/3/19	Collector	87	11.18	0.64	243459	-12.2	-91	6.6
10/31/19	Collector	30	0.01	0.24	243505	-11.6	-82	10.8
1/3/20	Collector	70	-3.21	0.11	243652	-17	-126	10.0
1/3/20	Bucket	71	-3.21	0.11	243653	-15.7	-119	6.6
2/2/20	Collector	32	-3.31	0.08	251702	-21	-164	4.0
3/2/20	Collector	41	-3.22	0.16	251703	-17.1	-135	1.8
4/4/20	Collector	30	-1.01	0.25	243934	-14.7	-109	8.6
5/3/20	Collector	46	3.39	0.42	244974	-16.8	-131	3.4
6/2/20	Collector	75	8.52	0.50	246039	-12.2	-97	0.6
6/29/20	Collector	102	12.34	0.65	246389	-15.9	-124	3.2
8/1/20	Collector	125	15.82	1.15	248474	-18.1	-145	-0.2
8/31/20	Collector	3.5	17.00	1.39	249598	-7.1	-67	-10.2
10/2/20	Collector	22	11.47	0.92	251701	-14	-109	3.0
11/1/20	Collector	97	2.70	0.41	251798	-14	-100	12.0
12/2/20	Collector	32	-2.26	0.14	251903	-20.2	-150	11.6
12/2/20	Bucket	33	-2.26	0.14	251904	-19.7	-148	9.6
1/2/21	Bucket	26	-4.86	0.10	252130	-16.4	-129	2.2
2/2/21	Bucket	10	-4.15	0.12	252131	-12	-120	-24.0
3/2/21	Bucket	88	-8.10	0.10	252200	-18.6	-147	1.8
4/2/21	Collector	27	0.04	0.29	252201	-20	-155	5.0

Sample Date	Method	Precipitation (mm)	Temp average °C	Vapor Pressure (kPa)	Sample ID	$d^{18}O$ ‰	$d^{2}H$ ‰	*d-excess*
4/2/21	Bucket	10	0.04	0.29	252203	-6.9	-94	-38.8
5/2/21	Collector	34	3.49	0.47	252301	-16.3	-124	6.4
6/2/21	Collector	64	7.63	0.61	252539	-18.2	-137	8.6
7/1/21	Collector	12	15.80	1.22	252554	-11.9	-98	-2.8
7/30/21	Collector	5	19.95	1.78	252921	-3.8	-54	-23.6
9/1/21	Collector	40	15.76	1.09	252918	-13.7	-107	2.6
10/1/21	Collector	15	11.07	0.90	253115	-10.5	-81	3.0
11/2/21	Collector	24	4.70	0.43	253121	-15.7	-121	4.6
11/30/21	Collector	37	0.20	0.18	253256	-16	-118	10.0
11/30/21	Bucket	37	0.20	0.18	253257	-12.5	-99	1.0
1/1/22			-5.11	0.09		No sample		
2/2/22	Collector	88	-6.78	0.10	253427	-21.8	-163	11.4
2/2/22	Bucket	88	-6.78	0.10	253428	-22.7	-169	12.6
3/1/22	Collector	41	-4.99	0.20	253433	-17.8	-134	8.4
3/1/22	Bucket	39	-4.99	0.20	253434	-16.5	-126	6.0
4/1/22	Collector	17	0.75	0.31	253585	-15.3	-121	1.4
4/28/22	Collector	22	0.54	0.33		No sample		
5/30/22	Collector	42	7.11	0.46	253743	-14.7	-115	2.6
6/24/22	Collector	56	12.14	0.60	253741	-13.9	-109	2.2
7/29/22	Collector	42	17.76	1.22	254014	-10.5	-91	-7.0
8/31/22	Collector	12	23.98	2.43	254019	-6.3	-63	-12.6
10/2/22	Collector	46	11.31	0.67	255165	-15.4	-115	8.2
10/31/22	Collector	22	6.27	0.41	255171	-20.4	-158	5.2
11/30/22	Collector	46	-7.82	0.10	255220	-23.5	-177	11.0
BITTERROOT-LOLO WATERSHED								
Lower Lolo: GNIP station 7277302, GWIC ID 292006, 46.74824, 114.13388, 998 m								
11/29/18	Collector	72	-0.48	0.25	236445	-18.3	-140	6.4
12/31/18	Collector	28	-3.41	0.14	237483	-19.8	-154	4.4
2/2/19	Collector	32	-3.79	0.21	238600	-20.2	-154	7.6
3/3/19	Collector	52	-8.24	0.05	238668	-25.2	-196	5.6
3/30/19	Collector	22	-0.38	0.17	238729	-19.5	-152	4.0
4/30/19	Collector	80	6.04	0.33	238771	-19.9	-159	0.2
5/29/19	Collector	40	11.18	0.61	238874	-15.2	-126	-4.4
7/2/19	Collector	15	15.29	0.86	238989	-12.7	-110	-8.4
8/1/19	Collector	27	18.31	1.12	239121	-10	-85	-5.0
8/30/19	Collector	33	18.55	1.15	240379	-10.3	-86	-3.6
10/4/19	Collector	50	13.63	0.71	243460	-10.9	-85	2.2
10/31/19	Collector	23	1.92	0.26	243499	-11.9	-90	5.2
12/2/19	Collector	20	-1.01	0.13	243604	-15.3	-109	13.4
1/4/19	Collector	28	-2.08	0.10	243654	-14.6	-108	8.8
1/31/20	Collector	18	-0.74	0.11	243792	-16.6	-127	5.8
2/29/20	Collector	60	-1.15	0.19	243848	-19	-146	6.0
4/4/20	Collector	28	1.78	0.33	243933	-16.5	-123	9.0
5/2/20	Collector	54	5.90	0.50	244973	-15.3	-120	2.4

Sample Date	Method	Precipitation (mm)	Temp average °C	Vapor Pressure (kPa)	Sample ID	$d^{18}O$ ‰	$d^{2}H$ ‰	*d-excess*
5/30/20	Collector	85	10.61	0.58	246038	-13.7	-107	2.6
7/2/20	Collector	81	14.15	0.73	246392	-17.7	-139	2.6
8/1/20	Collector	14.3	18.29	1.24	248476	-12.7	-102	-0.4
8/31/20	Collector	4.5	19.49	1.48	249595	-5.5	-52	-8.0
9/30/20	Collector	30	12.90	0.86	251700	-8.8	-93	-22.6
11/4/20	Collector	77	5.01	0.42	251768	-11.1	-79	9.8
Upper Lolo: GNIP station 7277303, GWIC ID 292026, 46.74652, 114.51642, 1,241 m								
11/29/18	Collector	65	-1.3	0.52	236446	-19	-144	8.0
12/31/18	Collector	52	-4.64	0.43	237481	-17.7	-136	5.6
2/2/19	Collector	39	-4.2	0.43	238598	-19.4	-147	8.2
3/3/19	Collector	75	-9.89	0.28	238669	-25.6	-198	6.8
3/30/19	Collector	20	-3.96	0.38	238728	-19.9	-155	4.2
4/30/19	Collector	101	3.3	0.63	238772	-20.2	-159	2.6
5/29/19	Collector	65	8.1	0.70	238872	-16.3	-129	1.4
7/2/19	Collector	20	12.17	0.73	238988	-13.6	-110	-1.2
8/1/19	Collector	22	14.89	0.66	239119	-11.3	-90	0.4
8/30/19	Collector	30	15.15	0.68	240378	-11.9	-94	1.2
10/4/19	Collector	38	9.64	0.74	243462	-12.3	-94	4.4
10/31/19	Collector	28	0.26	0.77	243502	-10.9	-81	6.2
12/2/19	Collector	21	-1.8	0.77	243605	-14	-105	7.0
1/4/19	Collector	45	-2.3	0.89	243655	-14.8	-109	9.4
1/31/20	Collector	25	-2.05	0.91	243791	-17.3	-132	6.4
2/29/20	Collector	42	-2.97	0.41	243847	-17.2	-132	5.6
4/4/20	Collector	32	-9.85	0.39	243932	-16.2	-121	8.6
5/2/20	Collector	34	4.04	0.50	244972	-16.2	-126	3.6
5/30/20	Collector	103	7.81	0.71	246037	-14.1	-107	5.8
7/2/20	Collector	88	11.73	0.93	246391	-16.8	-130	4.4
8/1/20	Collector	12.3	15.13	0.64	248473	-14.7	-115	2.6
8/31/20	Collector	28	15.17	0.62	249596	-8	-58	6.0
9/30/20	Collector	39	9.6	0.72	251699	-14.9	-115	4.2
11/4/20	Collector	76	2.9	0.80	251767	-8	-78	-14.0
Lolo Pass SNOTEL: GNIP station 7277304, GWIC ID 292585-Collector 304000-Bucket, 46.6378, 114.58139, 1,673 m								
11/29/18	Collector	169	-1.3		236437	-16.6	-120	12.8
12/31/18	Collector	100	-4.2		237488	-16.3	-121	9.4
12/31/18	Bucket	125	-4.2		237489	-16.2	-119	10.6
2/2/19	Collector	87	-3.42		238594	-17.7	-132	9.6
2/2/19	Bucket	130	-3.42		238595	-18.1	-137	7.8
3/3/19	Collector	99	-9.29		238670	-24.5	-187	9.0
3/3/19	Bucket	180	-9.29		238671	-25.2	-194	7.6
3/30/19	Collector	46	-1.26		238725	-19.8	-152	6.4
3/30/19	Bucket	N/A	-1.26		238726	-22.2	-171	6.6
4/30/19	Collector	210	2.92		238773	-18.3	-143	3.4
5/29/19	Collector	59	7.33		238870	-19.1	-150	2.8

Sample Date	Method	Precipitation (mm)	Temp average °C	Vapor Pressure (kPa)	Sample ID	$d^{18}O$ ‰	$d^{2}H$ ‰	*d-excess*
7/2/19	Collector	11	11.39		238987	-8.5	-90	-22.0
8/1/19	Collector	16	14.79		239115	-8.7	-77	-7.4
8/30/19	Collector	40	14.52		240377	-9.2	-82	-8.4
10/4/19	Collector	72	9.21		243465	-11.9	-86	9.2
10/31/19	Collector	120	0.18		243501	-13.3	-93	13.4
12/2/19	Collector	62	-1.33		243601	-14.8	-114	4.4
12/2/19	Bucket	62	-1.33		243602	-14.7	-104	13.6
1/4/20	Collector	139	-2.08		243656	-14.4	-104	11.2
1/4/19	Bucket	145	-2.08		243657	-15.5	-112	12.0
1/30/20	Collector	130	-2.56		243788	-16.6	-122	10.8
1/30/20	Bucket	213	-2.56		243789	-18.1	-133	11.8
2/29/20	Collector	137	-3.25		243840	-15.6	-114	10.8
2/29/20	Bucket	155	-3.25		243841	-17	-125	11.0
4/4/20	Collector	102	-1.16		243929	-15.9	-118	9.2
4/4/20	Bucket	110	-1.16		243930	-15.8	-117	9.4
5/2/20	Collector	78	3.44		244970	-14.8	-113	5.4
5/30/20	Collector	126	6.39		246036	-15.1	-113	7.8
7/2/20	Collector	145	10.51		246390	-17.7	-133	8.6
8/1/20	Collector	13.5	15		248475	-15.1	-116	4.8
8/31/20	Collector	18	15		249597	-9.3	-69	5.4
9/30/20	Collector	63	11		251698	-13.5	-98	10.0
11/1/20	Collector	161	3.53		251766	-13.6	-95	13.8
12/2/20	Collector	158	-1.26		251899	-17.4	-124	15.2
12/31/20	Bucket	147	-2.98		251900	-17.8	-127	15.4
1/30/21	Bucket	118	-3.13		252127	-17	-129	7.0
2/26/21	Bucket	126	-4.15		252128	-17.7	-136	5.6
4/2/21	Collector	75	-0.33		252196	-16.2	-121	8.6
4/2/21	Bucket	75	-0.33		252197	-14.1	-118	-5.2
4/30/21	Collector	48	2.65		252293	-16.4	-125	6.2
5/30/21	Collector	87	5.98		252536	-17.8	-135	7.4
6/29/21	Collector	48	13.89		252550	-12.4	-90	9.2
8/3/21	Collector	10	18.65		252841	-9.1	-83	-10.2
8/29/21	Collector	29	13.51		252842	-12.9	-101	2.2
9/30/21	Collector	43	10.62		253114	-14	-101	11.0
10/29/21	Collector	90	4.6		253123	-16.7	-128	5.6
12/1/21	Collector	99	0.56		253254	-15.3	-110	12.4
12/1/21	Bucket	99	0.56		253255	-15.3	-109	13.4
12/30/21	Bucket	195	-3		253586	-19.1	-140	12.8
1/31/22	Bucket	181	-3.89		253436	-19.9	-146	13.2
1/31/22	Bucket	181	-3.89		253587	-19.3	-143	11.4
2/21/22	Bucket	126	-1.85		253588	-17.5	-130	10.0
3/31/22	Collector	73	0.31		253591	-17.6	-132	8.8
3/31/22	Bucket	71	0.189		253592	-16.8	-127	7.4
5/2/22	Collector	46	0.22		253594	-16.8	-127	7.4
5/31/22	Collector	114	4.92		253595	-16.3	-125	5.4

Sample Date	Method	Precipitation (mm)	Temp average °C	Vapor Pressure (kPa)	Sample ID	$d^{18}O$ ‰	$d^{2}H$ ‰	*d-excess*
6/27/22	Collector	147	9.75		254011	-16.5	-127	5.0
7/28/22	Collector	113	16.73		254016	-11.1	-89	-0.2
8/31/22	Collector	26	17.24		254030	-7	-64	-8.0
10/4/22	Collector	53	11.86		255169	-9.7	-120	-42.4
11/1/22	Collector	70	6.05		255170	-17.1	-132	4.8
11/30/22	Collector	92	-4.64		255219	-17.6	-155	-14.2

Note. Error notation: D and WD, duplicates collected, only one used; E, specific source of error undetermined; PDE, low precipitation resulting in post-depositon evaporation; SE, sampling methodology error.

APPENDIX B: SITE SCHEDULE FOR BOTTLE AND DELIVERY MECHANISM EXCHANGE

Appendix B. Site schedule for bottle and delivery mechanism exchange.

Basin/Site	Small Bottle	Siphon In	Siphon Out
Upper Clark Fork			
Basic Creek SNOTEL	June–July	October 1st	April 1st
MBMG	All Year	October 1st	April 1st
Upper Missouri			
MacDonald Pass	June–August	October 1st	April 1st
Helena Valley	All Year	October 1st	April 1st
Blackfoot			
Lubrecht	May–August	October 1st	March 1st
Bitterroot–Lolo Watershed			
Lolo Pass SNOTEL	May–August	October 1st	April 1st
Upper Lolo	May–August	October 1st	April 1st
Lower Lolo	May–August	October 1st	March 1st

APPENDIX C: TRITIUM VALUES

Appendix C. Tritium values.

Site Name	GWIC No.	Sample ID	Sample Date	Collection Month	Season[1]	Method	Tritium (TU)
Basin Creek SNOTEL	298870	243507	11/2/19	Oct–19	Fall_Early Winter	Collector	7.0
Basin Creek SNOTEL	298870	251777	11/1/20	Oct–20	Fall_Early Winter	Collector	4.7
Basin Creek SNOTEL	298870	251902	11/28/20	Nov–20	Fall_Early Winter	Collector	7.4
Basin Creek SNOTEL	304005	251907	12/30/20	Dec–20	Fall_Early Winter	Bucket	6.6
MacPass	298420	236439	11/1/18	Oct–18	Fall_Early Winter	Collector	7.3
MacPass	298420	238779	11/2/19	Oct–19	Fall_Early Winter	Collector	6.8
Lubrecht Jones Pond	297503	236442	11/1/18	Oct–18	Fall_Early Winter	Collector	3.7
Lolo Pass SNOTEL	292585	236437	10/31/18	Oct–18	Fall_Early Winter	Collector	4.0
Lolo Pass SNOTEL	292585	238987	10/31/19	Oct–19	Fall_Early Winter	Collector	3.0
Lolo Pass SNOTEL	292585	251766	11/1/20	Oct–20	Fall_Early Winter	Collector	3.8
Lolo Pass SNOTEL	292585	251899	12/2/20	Nov–20	Fall_Early Winter	Collector	5.0
Lolo Pass SNOTEL	304000	251900	12/31/20	Dec–20	Fall_Early Winter	Bucket	4.6
Lolo Pass SNOTEL	304000	252127	1/30/21	Jan–21	Fall_Early Winter	Bucket	3.9
Basin Creek SNOTEL	298870	251696	9/28/20	Sep–20	Shoulder	Collector	7.7
Basin Creek SNOTEL	304005	252138	2/25/21	Feb–21	Shoulder	Bucket	7.0
Basin Creek SNOTEL	298870	252839	8/2/21	Jul–21	Shoulder	Collector	13.1
Basin Creek SNOTEL	298870	252844	9/1/21	Aug–21	Shoulder	Collector	9.4
Lolo Pass SNOTEL	292585	249597	8/31/20	Aug–20	Shoulder	Collector	8.3
Lolo Pass SNOTEL	292585	251698	9/30/20	Sep–20	Shoulder	Collector	5.3
Lolo Pass SNOTEL	304000	252128	2/26/21	Feb–21	Shoulder	Bucket	4.7
Lolo Pass SNOTEL	292585	252841	8/29/21	Aug–21	Shoulder	Collector	6.3
Basin Creek SNOTEL	298870	238882	6/1/19	May–19	Spring_Early Summer	Collector	15.6
Basin Creek SNOTEL	298870	246032	6/1/20	May–20	Spring_Early Summer	Collector	9.8
Basin Creek SNOTEL	298870	252194	3/31/21	Mar–21	Spring_Early Summer	Collector	11.4
Basin Creek SNOTEL	298870	252296	5/1/21	Apr–21	Spring_Early Summer	Collector	13.3
Basin Creek SNOTEL	298870	252538	6/1/21	May–21	Spring_Early Summer	Collector	12.8
MacPass	304011	238588	5/31/19	May–19	Spring_Early Summer	Collector	14.9
MacPass	298420	243593	6/2/20	May–20	Spring_Early Summer	Collector	10.3
Lolo Pass SNOTEL	292585	238773	3/30/19	Mar–19	Spring_Early Summer	Collector	5.2
Lolo Pass SNOTEL	292585	238773	4/30/19	Apr–19	Spring_Early Summer	Collector	5.9
Lolo Pass SNOTEL	292585	246036	5/30/20	May–20	Spring_Early Summer	Collector	10.3
Lolo Pass SNOTEL	292585	252196	4/2/21	Mar–21	Spring_Early Summer	Collector	8.5
Lolo Pass SNOTEL	292585	252293	4/30/21	Apr–21	Spring_Early Summer	Collector	11.0
Lolo Pass SNOTEL	292585	252536	5/30/21	May–21	Spring_Early Summer	Collector	10.9
Lolo Pass SNOTEL	292585	252550	6/29/21	Jun–21	Spring_Early Summer	Collector	13.8
Lolo Pass SNOTEL	298883	428660	3/30/19	Mar–19		Snowpack	5.2

[1]Spring through early summer (March–June), fall through early winter (October–January).

APPENDIX D: DATA ANALYSIS METHODS USED TO IDENTIFY ERRORS

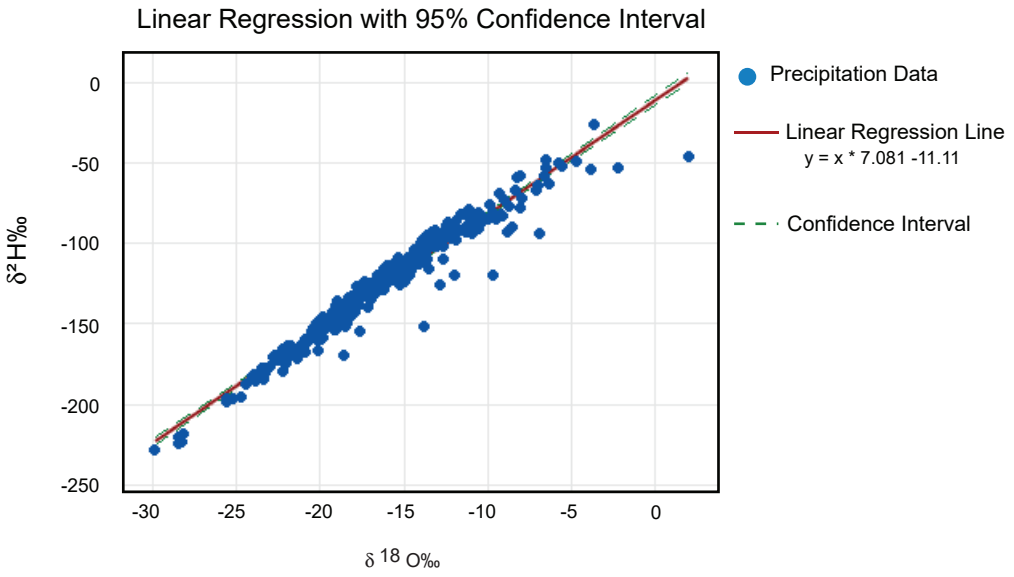

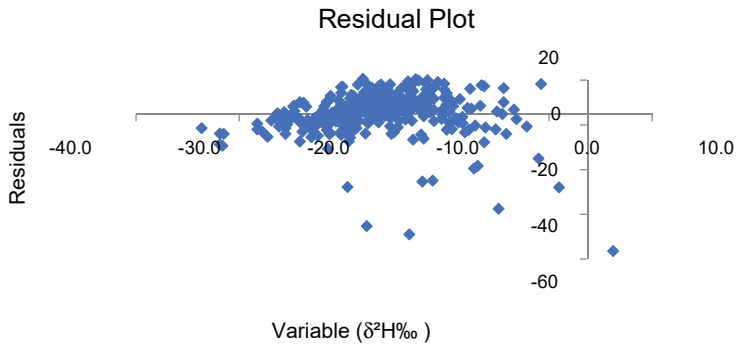

Residual Shapiro Test: $2.2e^{-16}$

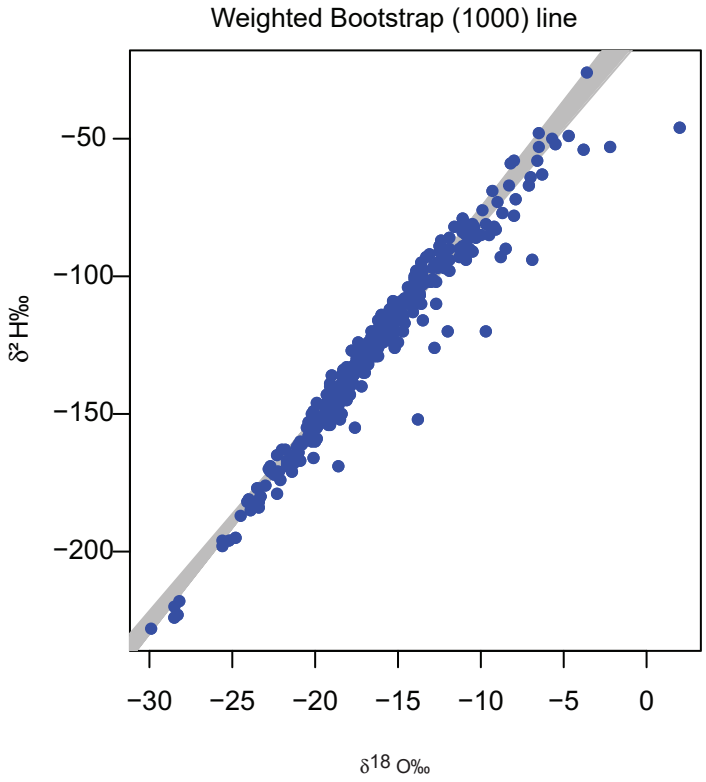

APPENDIX E: GRAPH OF SITE $\delta^{18}O$ DATA BY BASIN

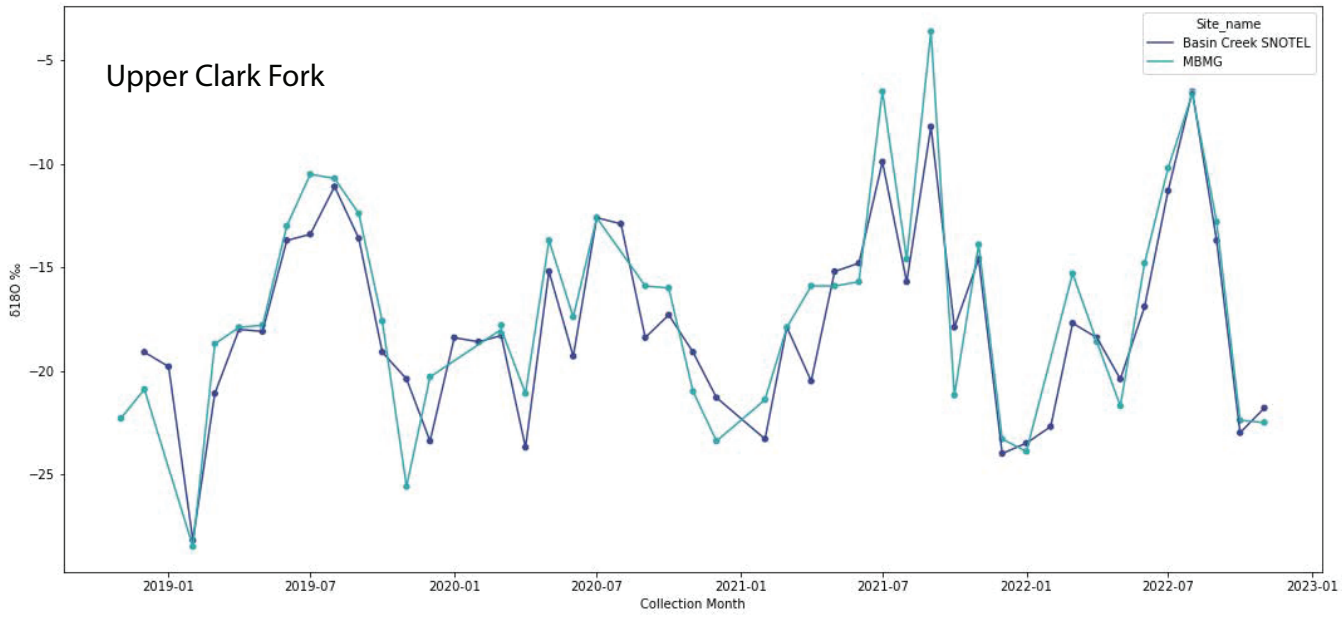
Upper Clark Fork
Site_name
Basin Creek SNOTEL
MBMG
δ18O ‰
Collection Month
2019-01
2019-07
2020-01
2020-07
2021-01
2021-07
2022-01
2022-07
2023-01

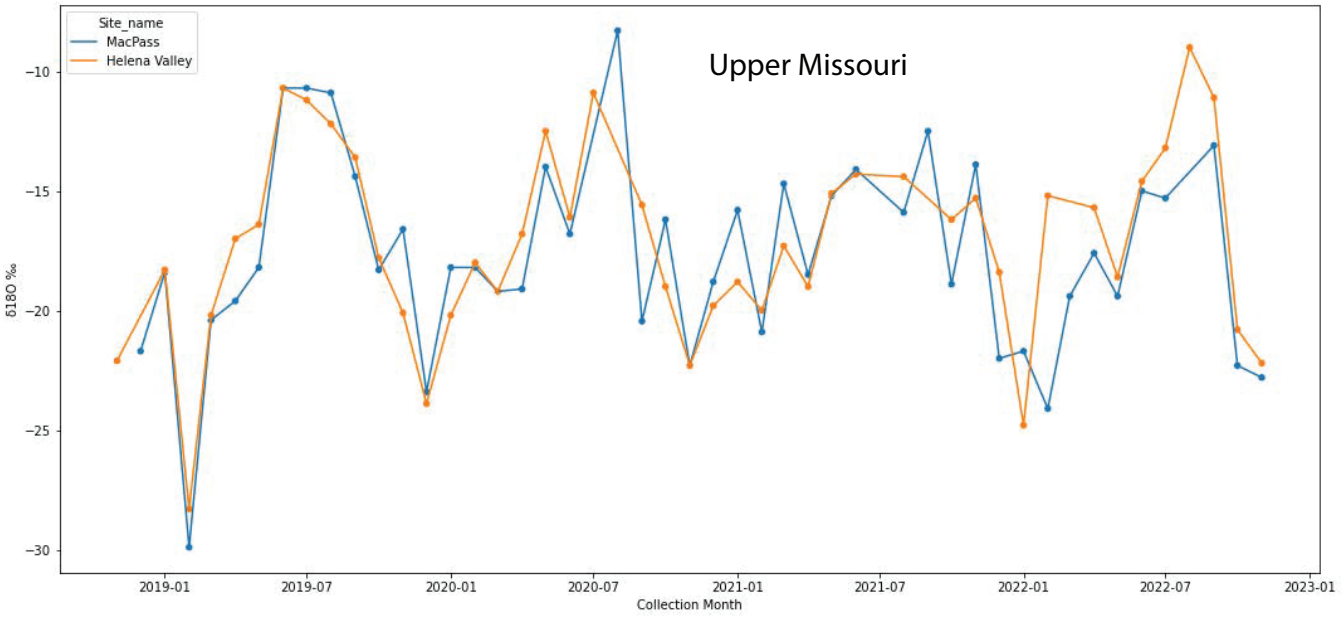
Upper Missouri
Site_name
MacPass
Helena Valley
δ18O ‰
Collection Month
2019-01
2019-07
2020-01
2020-07
2021-01
2021-07
2022-01
2022-07
2023-01

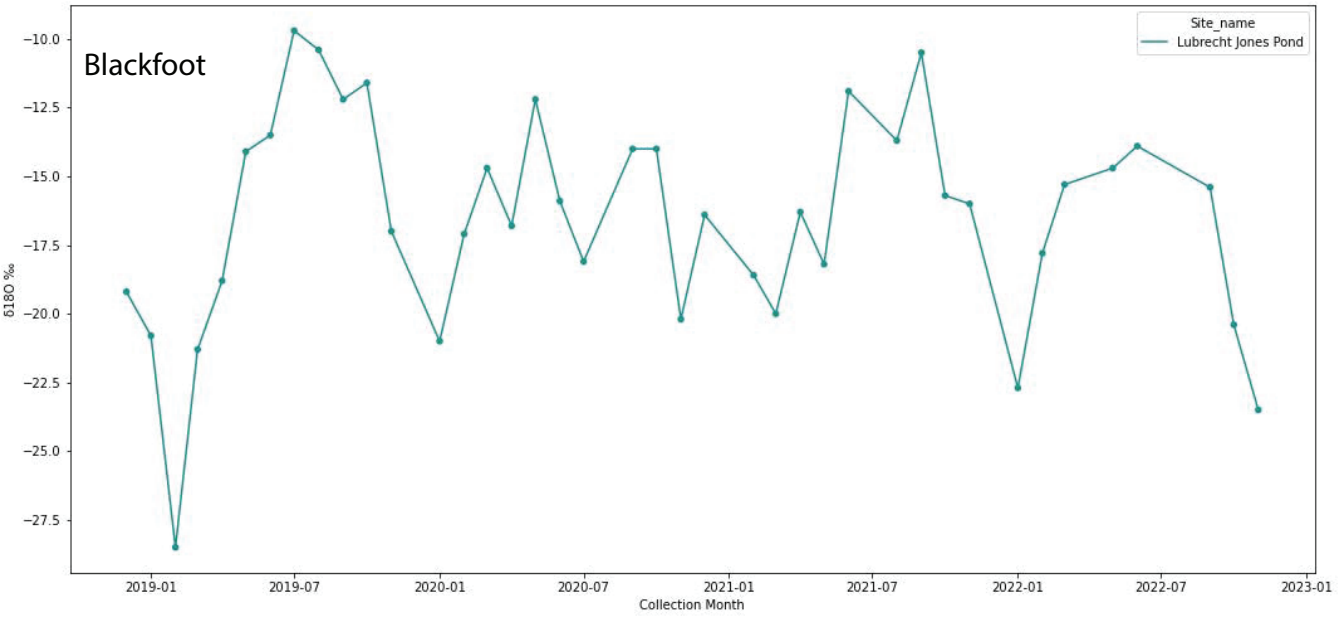
Blackfoot
Site_name
Lubrecht Jones Pond
δ18O ‰
Collection Month
2019-01
2019-07
2020-01
2020-07
2021-01
2021-07
2022-01
2022-07
2023-01